JOURNAL OF MATERIALS SCIENCE 27 (1992) 5113–5140

Review
Synthesis, properties and applications of titanium aluminides

F. H. FROES, C. SURYANARAYANA, D. ELIEZER*
Institute for Materials and Advanced Processes, College of Mines and Earth Resources, University of Idaho, Moscow, Idaho 83843-4195, USA

Attractive elevated-temperature properties and low density make the titanium aluminides very interesting for both engine and airframe applications, particularly in the aerospace industry. The challenge to the materials scientist is to maintain these characteristics while building-in "forgiveness". The basic phase diagram and crystal structure of both the Ti_3Al and TiAl phases are reviewed, followed by a consideration of chemistry–processing–microstructure–deformation/fracture–mechanical property relationships in monolithic material. Conventional and innovative synthesis methods are presented, including use of hydrogen as a temporary alloying element. Composite concepts as a method to enhance not only "forgiveness" but also elevated-temperature behaviour are discussed. Environmental effects are evaluated prior to consideration of present and projected applications of both monolithic and composite material. It is concluded that while the titanium aluminides in monolithic form can be used now in non-demanding applications, much further research and development is required before this material class can be used in critical applications, especially in composite concepts.

1. Introduction

Advanced materials are key to technological advancement [1, 2], and enhanced structural materials are particularly vital to aerospace system improvements where the extremely demanding conditions require that the new materials are "stronger, stiffer, hotter and lighter". These advanced materials will often be "tailored" or "engineered" to exhibit the properties required for a given application by use of composite concepts [3–17]. Cost can be a major concern, but an integrated design, manufacturing and use approach can lead to cost-effective application, where these new materials are considered as structures rather than in the same way as traditional materials such as metals.

An attractive class of "advanced materials" are the intermetallic compounds [18] which can be simply defined as an ordered alloy phase formed between two metallic elements [19], where an alloy phase is ordered if two or more sublattices are required to describe its atomic structure [20, 21]. The ordered structure exhibits attractive elevated-temperature properties (strength, stiffness, environmental resistance, etc.) because of the long-range ordered superlattice which reduces dislocation mobility and diffusion processes at elevated temperatures [22–25]. However, this reduced dislocation motion also results in generally extremely low ambient-temperature fracture-related properties including ductility and fracture toughness. Recent research has focused on understanding and controlling this brittleness while maintaining the attractive elevated-temperature characteristics.

Because of their low density the ordered intermetallic titanium aluminides, based on Ti_xAl ($x = 1$ or 3), are particularly attractive candidates for applications in advanced aerospace engine and airframe components, in both monolithic and composite concepts [26–33]. A comparison of the characteristics of the monolithic titanium aluminides with other aluminides is shown in Table I [34] and with conventional titanium alloys in the creep curves shown in Fig. 1 [9]. The present materials mix in an advanced jet engine is shown in Fig. 2 [34] and a possible material mix in a 2010 engine in Table II [34]. A

TABLE I Melting points and densities for aluminides [34]

Aluminide	Melting point (°C)	Density ($g\,cm^{-3}$)
Ti_3Al	1600	4.2
TiAl	1460	3.9
Fe_3Al	1540	6.7
FeAl	1330	5.6
Ni_3Al	1390	7.5
NiAl	1640	5.9
Superalloys (typical)	1325–1400	9

---

* On leave from Ben Gurion University of the Negev, Beer Sheva, Israel.

0022–2461 © 1992 Chapman & Hall

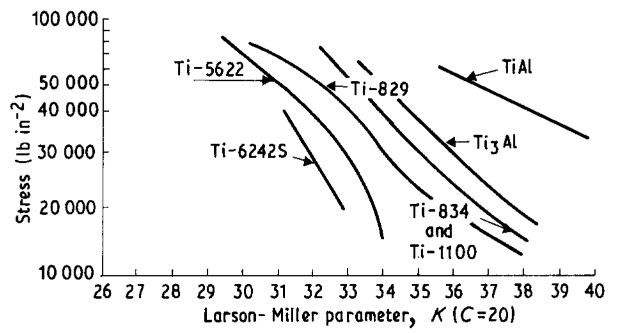

Figure 1 Comparison of the creep behaviour (0.2% creep strength) of terminal and intermetallic titanium-based alloys [9]. 1 lb in^{-2} = 703 kg m^{-2}.

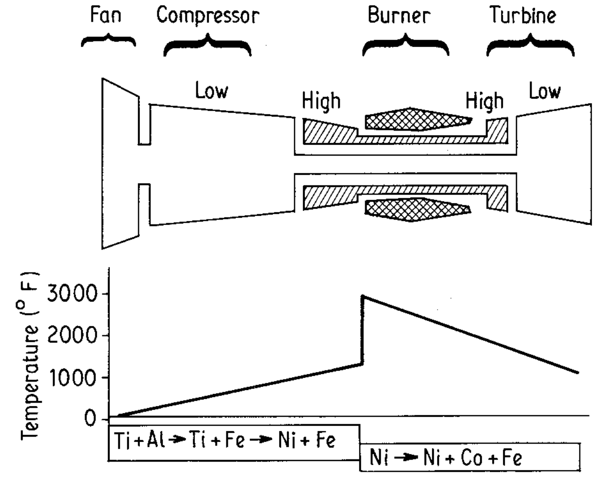

Figure 2 Material mix in a current advanced turbofan engine [34]. °C = (°F − 32)/1.8.

TABLE II Possible aircraft engine material mix in 2010 [34]

Material	Percentage
Metal matrix composites	30
Ceramics (aluminides) and ceramic composites	30
Superalloys	13
Resin (polymer) composites	10
Titanium	10
Steel	7
Aluminium	0
Magnesium	0

summary of the properties of these aluminides is compared with those of conventional titanium alloys and superalloys in Table III [27–35]. A further negative feature is that oxidation resistance is lower than desirable at elevated temperatures [36–38]; thus, a key factor in increasing the maximum use temperature is enhanced oxidation resistance while maintaining creep and strength performance. A separate section will address environmental effects.

Composite concepts using the titanium aluminides as a matrix are being actively pursued [12, 39–42], to increase "forgiveness" and enhance elevated-temperature performance, particularly modulus; and these will be discussed.

The system "pull" exerted in the USA by the National Aerospace Plane (NASP), Integrated High Performance Turbine Engine Technology (IHPTET) programs, and other advanced aerospace concepts, has caused an explosion in open-literature publications on the titanium aluminides. We will draw heavily on the many review papers, conference proceedings [27, 31–33, 39–47], and research papers that have appeared recently addressing intermetallics in general and the titanium aluminides specifically.

2. Phase diagrams

Alloys based on TiAl have been under development since 1955 [48] and those based on Ti_3Al since 1960 [49], but the strong effect of interstitial elements (oxygen and hydrogen) has hampered determination of an accurate Ti–Al phase diagram. Using earlier literature [50–60], and also thermodynamic modelling, Murray [61, 62] proposed a comprehensive binary Ti–Al phase diagram which includes Ti_3Al (α_2), TiAl (γ), $TiAl_2$, δ and $TiAl_3$ intermediate phases, and α-Ti, β-Ti and α-Al terminal solid solutions. However, neither the invariant reaction temperatures nor some phase boundaries, such as $\alpha_2/\alpha_2 + \gamma/\gamma$, have been accurately defined. Further, Murray predicts that a Ti–50 at % Al* alloy will solidify as cubic dendrites of β surrounded by γ formed according to the peritectic reaction $L + \beta \rightarrow \gamma$. At lower Al contents and at lower temperatures, the α phase forms from the β and γ phases by a peritectoid reaction, with subsequent α decomposition taking place eutectoidally to a lamellar

TABLE III Properties of titanium aluminides, titanium-base conventional alloys and superalloys [28–35]

Property	Ti base	Ti_3Al base	TiAl base	Superalloys
Density (g cm^{-3})	4.5	4.1–4.7	3.7–3.9	8.3
Modulus (GPa)	96–100	100–145	160–176	206
Yield strength (MPa)	380–1150	700–990	400–650	–
Tensile strength (MPa)	480–1200	800–1140	450–800	–
Creep limit (°C)	600	760	1000	1090
Oxidation limit (°C)	600	650	900	1090
Ductility at RT (%)	20	2–10	1–4	3–5
Ductility at HT (%)	High	10–20	10–60	10–20
Structure	A3/A2	DO_{19}	$L1_0$	f.c.c./$L1_2$

---

*Throughout the text all compositions are expressed in at % unless otherwise stated.

$\alpha_2 + \gamma$ structure. In fact recent results from both ingot metallurgy [63, 64] and rapid solidification [65] routes indicate that around 50% Al the α phase forms directly from the liquid state according to the peritectic reaction $L + \beta \rightarrow \alpha$; and the presently accepted version of the Ti–Al phase diagram is shown in Fig. 3 [66].

The Ti_3Al phase undergoes a disorder–order transformation in the range of 22 to 39% Al and congruently at 1180 °C. The ordered α_2 phase has a hexagonal structure with $a = 0.5782$ nm and $c = 0.4629$ nm. The TiAl (γ) phase, stable from 49 to 66% Al, is considered to be ordered up to the melting point, although this is not certain [67] because antiphase boundaries were observed in rapidly solidified Ti–60% Al alloy. The γ phase has an ordered face-centred tetragonal structure with $a = 0.4005$ nm and $c = 0.4070$ nm, and a tetragonality of only 1.02 at the equiatomic position which increases to 1.03 at higher Al contents.

Additions of β-stabilizing elements such as Nb, Mo, V and Ta enhance room-temperature ductility, and much work is in progress to establish the constitution of ternary Ti–Al–M (M = Nb, V, Mo, Ta, Mn, etc.) systems [68–74], with emphasis on Ti–Al–Nb [73, 74]. In Ti–Al–Nb alloys containing 5 to 17 at % Nb a ductile ordered b.c.c. phase (B2) forms on quenching from high temperatures [75]; this also occurs in alloys containing other β-stabilizing elements [76, 77]. Additionally, an equilibrium ordered orthorhombic phase is detected in Ti–Al–Nb alloys with an approximate stoichiometry of Ti_2AlNb [78]. Alloys quenched from the high-temperature β phase (both in the binary and the ternary alloys) undergo a variety of martensitic transformations. Similarly, alloys containing the B2 phase form the ω and ω-related phases on cooling to room temperature from elevated temperatures >1100 °C [74, 79]. Table IV presents the crystal structure data of the stable and metastable phases detected to date in titanium-rich binary Ti–Al and ternary Ti–Al–Nb systems.

3. Specific systems

3.1. Ti_3Al (α_2)

3.1.1. Chemistry

Semi-commercial and experimental α_2 alloys developed to the present time are two-phase (α_2 + β/B2) with compositions based on Ti–(23–25)Al–(10–30)Nb [31–33, 82, 83]. Alloy compositions with current engineering significance are Ti–24Al–11Nb [83–85], Ti–25Al–10Nb–3V–1Mo [29, 83], Ti–25Al–17Nb–1Mo [83, 86] and Ti–23.5Al–24Nb [82]. Generally, increasing Nb content enhances the majority of the material properties [87] with the exception of creep performance. Nb, which substitutes for Ti atoms and increases the number of slip systems [88–90], may be replaced by specific elements for improved strength (Mo, Ta, Cr), creep resistance (Mo), and oxidation resistance (Ta, Mo). Good elevated-temperature strength, creep resistance and environmental resistance are favoured by high Al, a moderately high β-stabilizer addition, and low V [28, 29, 84–86, 91–93].

Care should be exercised in evaluating early work because of variations in composition, processing, microstructure, and testing procedures [87]. Of particular importance is oxygen level, which raises the ductile-to-brittle transition temperature of titanium alloys [87]. Reduction of oxygen content from 0.186 to 0.081 wt % for the Ti–24Al–11Nb alloy results in an increase in tensile elongation from 1.1% up to 4.8%

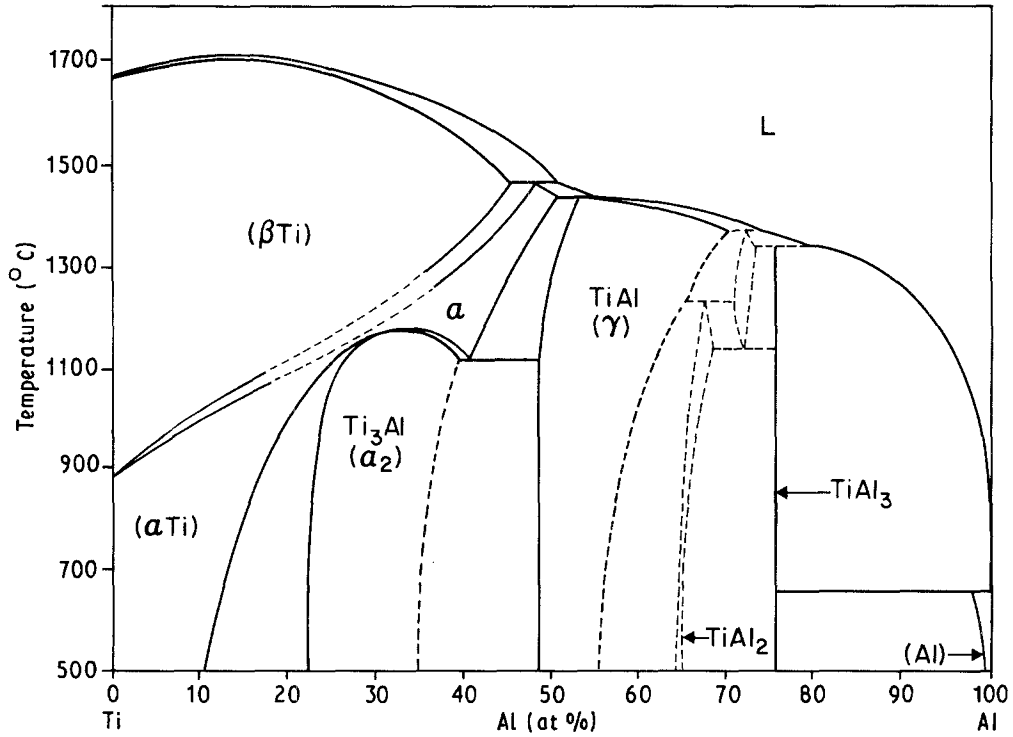

Figure 3 Schematic binary Ti–Al phase diagram [66].

TABLE IV Crystal structure data of the stable and metastable phases in titanium-rich Ti–Al and Ti–Al–Nb alloys

Phase	Strukturbericht symbol	Crystal structure	Space group	Pearson symbol	Lattice parameters (nm)			Reference
					a	b	c	
Ti (α)	A3	h.c.p.	$P6_3/mmc$	hP2	0.29508	–	0.46885	80
Ti (β)	A2	b.c.c.	Im3m	cI2	0.33132	–	–	80
$Ti_3Al(\alpha_2)$	DO_{19}	Ordered hexagonal	$P6_3/mmc$	hP8	0.5782	–	0.4629	80
TiAl(γ)	$L1_0$	Ordered f.c.c. tetragonal	P4/mmm	tP4	0.4005	–	0.4070	80
B2[a]	DO_3	Ordered b.c.c.	$Pm\bar{3}m$	cI2	0.322	–	–	
–	$B8_2$[b]	Hexagonal	$P6_3/mmc$	–	0.45803	–	0.55204	79
$Ti_2AlNb(O)$		Orthorhombic	Cmcm	–	0.45	0.588	0.960	78
					0.62	0.94	0.47	70
					0.596	0.986	0.467	81
ω[c]	–	Hexagonal	P6/mmm	–	0.46	–	0.58	79
ω″[c]	–	Trigonal	$P\bar{3}m1$	–	0.4555	–	0.5542	79

[a] Observed only in ternary Ti–Al–M alloys where M is a β-stabilizing element.

[b] Low-temperature equilibrium phase in Ti–Al–Nb alloys.

[c] Transitional phases formed during decomposition of the B2 phase.

[94], perhaps due to increased basal slip as the oxygen level decreases [95]. Additions of Y (discussed elsewhere) and B (up to 0.5%) can be used to control grain size [96]. Some interesting additions may have been prematurely abandoned; for example Zr, which when added at the 7–14% level showed attractive levels of strength and ductility [87].

3.1.2. Processing/microstructure development

Microstructural features that can be varied by thermomechanical processing (TMP) include the β grain morphology and distribution, primary α_2 grain size and volume fraction, and secondary α_2 plate morphology and thickness [31–32]. β processing generally results in elongated Widmanstatten α_2 in large primary β grains, while α–β processing results in more equiaxed primary α grains. Both microstructure and mechanical properties follow the behaviour of more conventional titanium alloys [26, 90], with the caveat that because of their ordered nature the Ti_3Al alloys are very brittle and fracture by a cleavage mechanism at ambient temperatures [97].

Generally transformed β microstructures (to produce elongated plate-like α_2) have been considered to be the optimum microstructure because this structure was considered necessary to achieve the best balance of room-temperature ductility and elevated-temperature properties [83, 84]. More recently, more equiaxed α_2 morphologies have been investigated because of their potential for increased room-temperature ductility [83, 98]. A small α_2 grain size enhances strength [90, 96]; and generally a refined slip length improves ductility levels, using either grain size, the allotropic change, or precipitation of second-phase particles [90]. An indication of the variety of microstructures which can be achieved is shown in Fig. 4 [82].

Until recently parameters such as ductility were influenced by (a) adjusting the amount of β phase by chemistry and heat-treatment or (b) by modifying the basic deformation mechanisms of the DO_{19} lattice of the α_2 [97], rather than by microstructure control. This appears to be a serious omission (see section 3.1.3 below).

3.1.3. Deformation and fracture

The deformation behaviour of Ti_3Al-based alloys has been reviewed [27, 83, 95], with the limited ductility at low temperatures attributed to the planarity of slip and the absence of slip in planes parallel to and/or inclined to the hexagonal axis [99], i.e. lack of an adequate number of independent slip systems. Ti_3Al (α_2) has a DO_{19} ordered hexagonal structure (Fig. 5a). An important difference in the deformation behaviour of Ti_3Al and other h.c.p. metals and alloys is the absence of twinning in Ti_3Al with slip being preferred. Long-range order suppresses twinning in Ti_3Al because such deformation produces disorder. The possible slip planes and directions are shown in Fig. 5b, from which it is apparent that three types of dislocation are possible:

(i) $\langle a \rangle$ type with a Burgers vector of the type $\frac{1}{6}\langle 1\,1\,\bar{2}\,0 \rangle$ moving on basal $(0\,0\,0\,1)$, prism $\{1\,0\,\bar{1}\,0\}$ or pyramidal $\{2\,0\,\bar{2}\,1\}$ planes;

(ii) $\langle c \rangle$ type with a Burgers vector of $[0\,0\,0\,1]$ on second-order $\{1\,1\,\bar{2}\,0\}$ prism planes, and

(iii) $\langle c + a \rangle$ type with a Burgers vector of $\langle 1\,1\,\bar{2}\,6 \rangle$ on $\{1\,1\,\bar{2}\,1\}$ or $\{2\,0\,\bar{2}\,1\}$ pyramidal planes.

However, on deformation at room and intermediate temperatures, only $\langle a \rangle$ type dislocations are observed in Ti_3Al alloys. The absence of c-component deformation results in generation of local stresses resulting in brittle cleavage and poor ductility. Deformation-induced twinning can produce the $\langle c \rangle$-type dislocations, but this mode of deformation is not possible at room temperature without causing disordering. Occurrence of microtwinning [27, 88] and the presence of $\langle c \rangle$ and $\langle c + a \rangle$ type dislocations in samples deformed at high temperatures [100–103] have been suggested as responsible for the increased ductility. $\langle c \rangle$

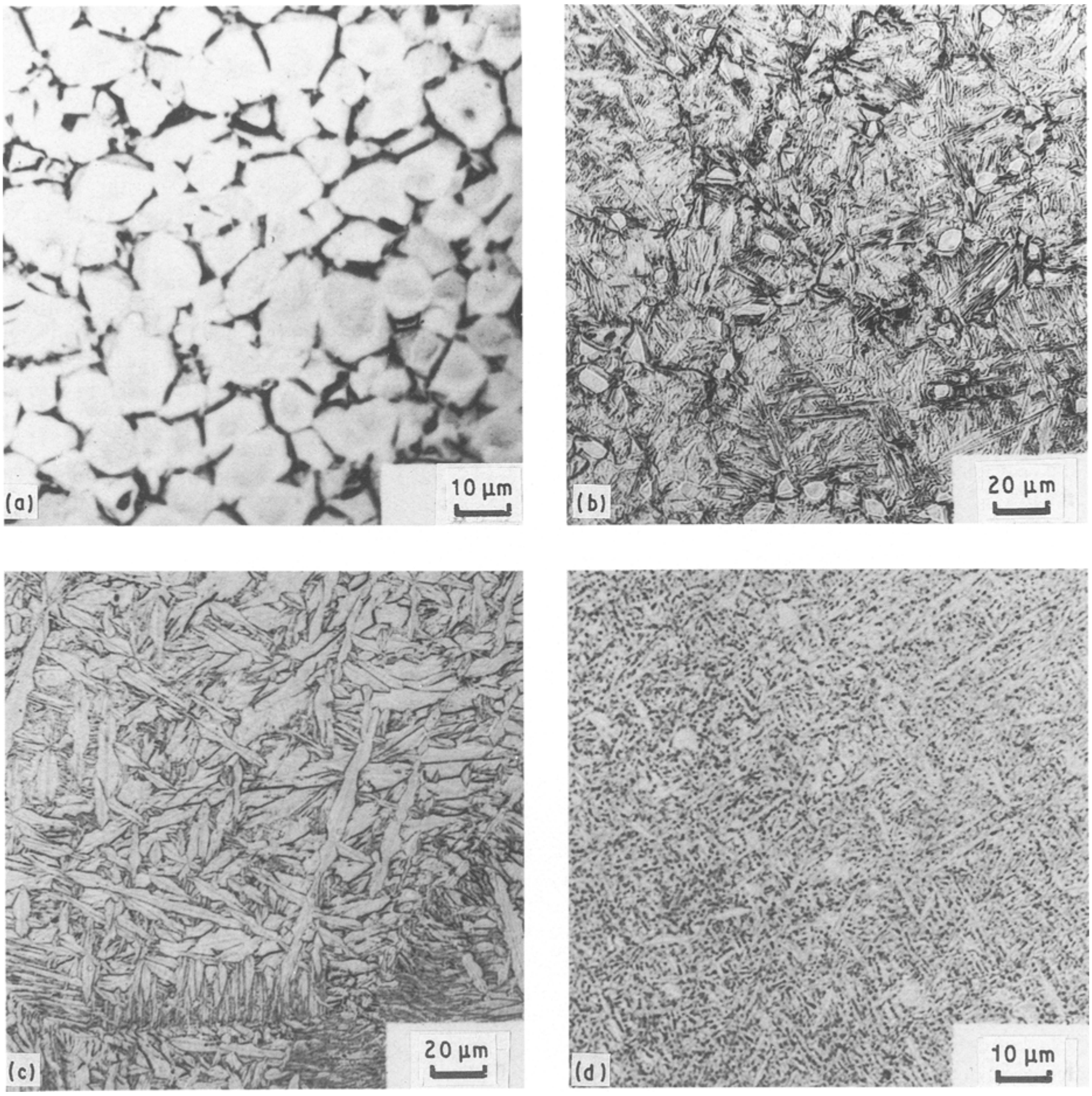

Figure 4 Microstructures developed in a Ti–25Al–7.5Nb alloy by transforming from the β phase: (a) equiaxed microstructure with a high volume fraction of primary α_2 phase, (b) low volume fraction of primary α_2 phase in a Widmanstatten transformed matrix, (c) coarse Widmanstatten transformed microstructure and (d) fine Widmanstatten transformed microstructure [82].

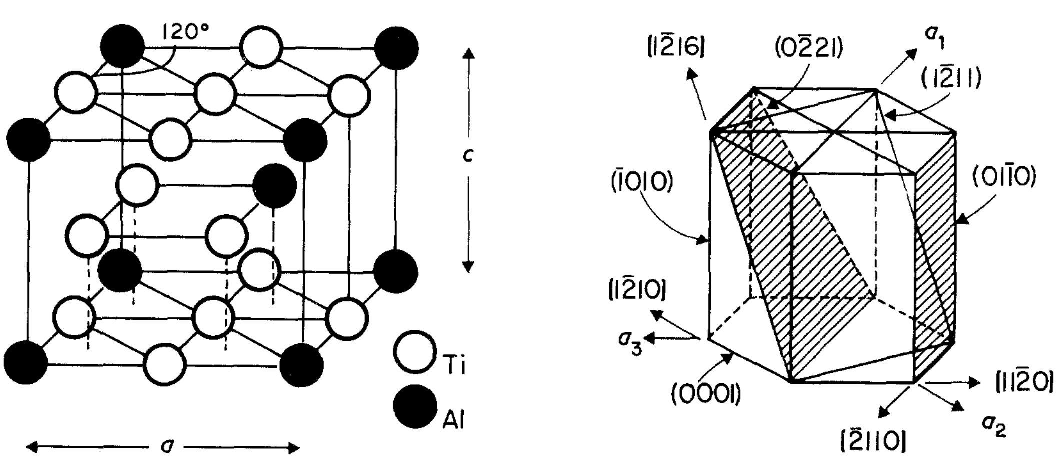

Figure 5 (a) Crystal structure of Ti_3Al (α_2) phase and (b) possible slip planes and slip vectors in the structure [31].

and $\langle c + a \rangle$ type dislocations have also been reported in samples deformed at room temperature [104, 105]; thus, it is not clear that the increased ductility at high temperatures is the result of increased $\langle c + a \rangle$ dislocation activity. However, it has been recently shown [95] that $\langle c \rangle$ dislocations are present in undeformed material whenever the α_2 phase has precipitated from the β phase; thus $\langle c \rangle$ dislocations are a transformation-induced rather than deformation-induced product. In addition, it has been suggested that the motion of these dislocations can only occur by climb [106]. In fact, a reduction in the density of $\langle c + a \rangle$ dislocations has been reported with increasing test temperature in Ti_3Al–Nb alloys [102]; this seems to be more predominant in alloys containing > 25Al [99].

The mechanism by which the ductility is improved with increasing Nb content is unclear. Since the $\langle c + a \rangle$ dislocation activity decreases with increasing temperature [102], a possibility is that Nb reduces the slip length by refining the microstructure and increasing the amount of the retained β phase [107]. The $\frac{1}{6}\langle 11\bar{2}0 \rangle$ superpartials could then transfer to the β phase to become $\frac{1}{2}\langle 111 \rangle$ dislocations according to the Burgers relationship $(0001)_{\alpha_2}//(110)_\beta$ and $[11\bar{2}0]_{\alpha_2}//[111]_\beta$.

About 10 vol% of the β phase (either in the disordered condition or as ordered B2) is generally present in Ti_3Al–Nb alloys and exhibits a variety of structural instabilities resulting in the formation of ω-type phases [75], which however do not seem to cause embrittlement [108]. A detailed study of the deformation behaviour of the B2 phase in Ti–24Al–11Nb alloy showed that it deformed inhomogeneously by $\langle 111 \rangle$ slip on $\{110\}$, $\{123\}$ and $\{112\}$ planes. The slip band structure is complex, consisting of segments of heavily pinned edge dislocations with periodic cross-slip of screw components on to secondary slip planes, with isolated observations of [1 0 0] slip [103, 109].

The yield strength has been experimentally verified [103] as obeying the rule of mixtures [110]

$$\sigma_y = \sum f_{i\alpha}\sigma_{i\alpha} + f_\beta \sigma_\beta$$

where $f_{i\alpha}$ and $\sigma_{i\alpha}$ are the volume fraction and yield strength, respectively, of the α_2 phase appearing as the identifiable constituent within the microstructure and f_β and σ_β are the volume fraction and yield strength of the β phase.

At room and intermediate temperatures, fracture in this alloy class occurs by cleavage. Primary α_2 particles have been observed to crack during a tensile test giving an effective drop in load-bearing area [98]. Even at higher temperatures, when the alloy exhibits some ductility, completely ductile fracture has not been observed [88]; instead intergranular cracking takes place, accommodating strain across grain boundaries.

The fracture behaviour in these alloys is related to slip behaviour in the α_2 phase and also to the presence of the β/B2 phase. The tensile properties of Ti_3Al–Nb alloys are critically dependent on the shape, distribution and volume fractions of the α_2 and B2 phases [95, 97, 98, 103, 111], with boundary strengthening playing a dominant role [97]. Widmanstatten secondary α_2 resulted in better ductility than microstructures with an aligned α_2 morphology, with aligned colonies acting as single units. Increasing the primary α_2 volume fraction (up to 30%) in a fine Widmanstatten microstructure in the Ti–25Al–10Nb–3V–1Mo alloy decreases the yield strength of the alloy due to a decrease in volume fraction of fine matrix. The ductility depends on both the distribution and volume fraction of the α_2 phase and peaks at 30–35% α_2, a trend which was attributed to the cracks which formed in the relatively large primary α_2. This behaviour apparently does not parallel that in conventional titanium alloys in which increasing the amount of equiaxed primary α enhances ductility. However, very recent work [112] has clearly shown that if an optimum amount of equiaxed α_2 grains are produced by thermomechanical processing, room-temperature ductility can be dramatically improved (to 26% elongation), removing the inconsistency with the behaviour of conventional titanium alloys. Grain-boundary α_2 allows easy crack propagation and increases strain incompatibility at the boundary.

In other work on the Ti–24Al–11Nb alloy [98] the maximum elongation, of close to 10% in $\alpha_2 + \beta$ processed material occurred at 30–35 vol% of the α_2 phase. Interestingly, this corresponds to the minimum in yield strength for fine α_2 plates with primary α_2 present [97]. Continuation of this work [95, 112] confirmed that $\alpha_2 + \beta$ processed material exhibited higher ductilities than β processed material. It was suggested that easy cracking in the primary α_2 regions dominated [112] with some evidence of cracking along α_2–β interfaces [95]; however, microcrack propagation across adjacent transformed β regions was difficult. Generally the authors concluded that the room-temperature deformation of Ti_3Al-based materials could be understood primarily on the basis of slip within the α_2. Optimum creep behaviour was suggested to be associated with a basket-weave α_2 microstructure with a minimum of β phase.

Crack propagation within the α_2 phase is relatively easy, again due to the difficulty of the $\langle c \rangle$ component slip. When a crack is initiated on the basal plane and activates co-planar $\langle a \rangle$ slip, large normal stresses near the crack tip are generated, which relax only when $\langle c + a \rangle$ slip is activated, and without which the cracks continue to grow in the α_2. The effectiveness of tough β phase in blunting and bridging cracks increases with temperature and this, at least partially, explains the increased ductility at higher temperatures.

The finer-scale structure obtained when stoichiometric α_2 is alloyed with β-stabilizers such as Nb, V or Mo, in combination with β regions forming a continuous layer surrounding α_2 grains, enhances ductility [95, 97, 98, 113]. However, much further work is required to fully optimize the microstructures for a combination of mechanical properties; the recent high ductility (26% room-temperature elongation) with an optimum amount of fine equiaxed primary α_2 emphasizing this point [112].

3.1.4. *Mechanical properties*

The mechanical properties of monolithic α_2 alloys, which have recently been summarized in an excellent overview article [83], depend on composition and the microstructure developed by thermomechanical processing [31, 32, 82, 83, 95, 97, 98, 112]. The composi-

TABLE V Typical room-temperature mechanical properties and elevated creep rupture life of α_2 [19, 31, 32, 82, 86, 112]

Alloy	YS (MPa)	UTS (MPa)	*El* (%)	K_{IC} (MPa m$^{1/2}$)	Creep rupture^a
Ti–25Al	538	538	0.3		
Ti–24Al–11Nb	787	824	0.7		44.7
	761	967	4.8		
Ti–24Al–14Nb	831	977	2.1		59.5
Ti–24Al–14Nb–3V–0.5Mo			26.0^b		
Ti–25Al–10Nb–3V–1Mo	825	1042	2.2	13.5	360
Ti–24.5Al–17Nb	952	1010	5.8	28.3	62
	705	940	10.0		
Ti–25Al–17Nb–1Mo	989	1133	3.4	20.9	476
Ti–15Al–22.5Nb	860	963	6.7	42.3	0.9
Ti–23.5Al–24Nb	960^c				

^{a} Hours at 650 °C/380 MPa.
^{b} Specially processed [112].
^{c} Estimated from microhardness [19].

tions evaluated span 0–30 equivalent Nb content with the majority of the mechanical properties improving with increasing Nb content, with the caveat that Nb may reduce creep resistance [31, 32]; although recent work suggests that richer Nb-containing alloys containing the orthorhombic (O) phase may be useful for elevated-temperature applications [82]. Typical mechanical properties of α_2 alloys are listed in Table V [31, 32, 82, 86], with the two-phase alloys exhibiting up to a doubling of strength due predominantly to boundary strengthening, with long-range order, solid-solution and texture effects also contributing [31, 32, 97].

Increasing the Al level and the amount of β-stabilizers both result in increased yield strengths. A fine Widmanstatten microstructure with a small amount of primary α_2 grains exhibits better ductility than microstructures with a coarse Widmanstatten microstructure, or an aligned acicular α_2 morphology [31, 32].

The fatigue properties of titanium alloys are strongly influenced by microstructure, with high-ductility alloys being optimum under low-cycle fatigue (LCF) conditions [114] as anticipated from work on conventional titanium alloys [26]. The low ductility exhibited in material with Widmanstatten α plates in $\alpha + \beta$ alloys is responsible for low elevated-temperature LCF strength. Early data [115] suggests that the fatigue crack growth rate (FCGR) is relatively insensitive to microstructure, although the coarse Widmanstatten microstructure exhibits the slowest FCGR at low stress intensities. Fracture toughness appears to depend on microstructure as well as alloy composition but the precise relationship is yet to be defined [31]. The decreased toughness of the Ti–25Al–10Nb–3V–1Mo alloy may result from an increase in Mo level [91] in conjunction with a higher strength level. The higher (17 at %) Nb levels appear to have the capability of combining toughness with strength and creep behaviour [83]. The Ti–15Al–22.5Nb alloy has the highest fracture toughness reported for an α_2-type alloy [86, 91] but the creep-rupture is poor. The extremely low Charpy impact strength levels of the titanium aluminides (2–3 J compared to ~ 25 J for conventional titanium alloys) is a major cause for concern in applications requiring foreign-object damage resistance such as blades [83].

For the alloys listed in Table V, microstructural effects on creep can be as significant as compositional variations [83]. Although compositional effects are not yet clear [83] a recent detailed investigation on the microstructure/creep behaviour of Ti–25Al–10Nb–3V–1Mo has shown that the colony-type microstructure is characterized by enhanced creep resistance over other microstructures [116]. The creep resistance of Ti–25Al–10Nb–3V–1Mo is raised by a factor of ten in the steady-state regime over the conventional titanium alloy Ti–1100 and two orders of magnitude over Ti–6Al–2Sn–4Zr–2Sn–Si (Ti–6242S) [116]. However, 0.4% creep strain is reached within 2 h. The elements Si and Zr appear to improve creep resistance [117], but the most significant increase is attained by increasing the Al content to 25% and limiting β-stabilizing elements to about 12% [85, 118]. However, the Ti–24.5Al–17Nb–1Mo alloy exhibits rupture life superior to other α_2 alloys [31]. A comparison of mechanical properties with conventional materials is given below in section 7.3.

3.2. TiAl (γ)

3.2.1. Chemistry

γ-TiAl alloys introduced to the present time are in the range Ti–(46–52)Al–(1–10)M, with M being at least one element from V, Cr, Mn, Nb, Ta, W and Mo [28, 30–32, 92, 93, 119–121]. These alloys can be divided into single-phase (γ) alloys and two-phase ($\gamma + \alpha_2$) alloys [30–32].

Single-phase γ alloys contain third alloying elements such as Nb or Ta that promote strengthening and additionally enhance oxidation resistance [122]. The role of third alloying elements in two-phase alloys is to raise ductility (V, Cr, Mn) [28, 30–32, 119, 121], oxidation resistance (Nb, Ta) [122], or combined properties [30–32]. Also, as with the α_2 alloys, interstitial oxygen content is critical; for example, in a two-phase Ti–48Al alloy the tensile elongation increased from 1.9 to 2.7% with an oxygen reduction from 0.08 to 0.03% [123].

3.2.2. *Processing/microstructure development*

The microstructure of the nominally γ alloys can be single-phase γ or, in slightly leaner compositions, two-phase $\gamma + \alpha_2$. Further, by appropriate thermomechanical processing (TMP) the morphology of the phases can be adjusted to be either lamellar or equiaxed, or a mixture of both morphologies [30–32, 124].

The lamellar structure can lead to an effective refinement of the microstructure and improved ductility either directly [119, 120] or in combination with fine recrystallized γ grains [121]. Improved ductility occurs at about 10 vol % α_2; when the α_2 phase content exceeds 20 vol % ductility can be degraded [120]. This is consistent with the fact that α_2 becomes increasingly more brittle with increasing Al content over 25% [84] and the α_2 plates have a composition of approximately 35%Al.

In two-phase alloys, the ratio of lamellar to equiaxed γ must also be controlled [29–33, 119, 120] along with their distribution [124]. A lamellar volume fraction of about 30% gives a reasonable combination of properties with good high-temperature creep resistance and acceptable tensile strength and usable ductility [29]. The optimum structure for enhanced ductility has been suggested to consist of adjacent regions of lamellar and equiaxed morphologies [33, 124]. TMP refines the microstructure when processing is conducted such that both the α and γ grains are recrystallized in the $(\alpha + \gamma)$ phase field. Grain morphology varies considerably depending on composition, solution treatment temperature and time, cooling rate, and stabilization temperature and time [30]. Examples of the types of microstructure which can be developed in TiAl are shown in Fig. 6.

The grain size decreases with reduced Al level and with additions of W [90], V, Mn and Cr [120, 121]. The number of annealing twins in the γ-phase increases as Al content decreases or when Mn or V levels are increased [120], while Cr additions increase the volume fraction of the lamellar structure [121]. Very recent results from material with an extremely small ("nanostructure-sized") grain structure have exhibited high room-temperature elongation up to 5% [125], clearly an area worthy of further study.

3.2.3. *Deformation and fracture (γ)*

The deformation behaviour of γ alloys is anisotropic and emphasizes the tetragonality (Fig. 7a), albeit low. The $L1_0$ alloys show an anomalous increase in flow stress as temperature increases, with an asymmetry of the peak position, similar to other ordered intermetallics with the $L1_2$ and B2 structures. This has been shown in single-crystal $Ti_{45}Al_{55}$ and polycrystalline $Ti_{40}Al_{55}Nb_5$ [126] and $Ti_{35}Al_{55}V_{10}$ [127] alloys. The dislocation behaviour was studied during the mid-1970s [128, 129], but only recently has detailed identification and behaviour study of the dislocations been carried out [130–132].

The ordered nature of TiAl (successive (0 0 2) planes are made up entirely of Ti and Al atoms) and its slight tetragonality have important implications for the available Burgers vectors and the different stacking faults produced by partial dislocations. The

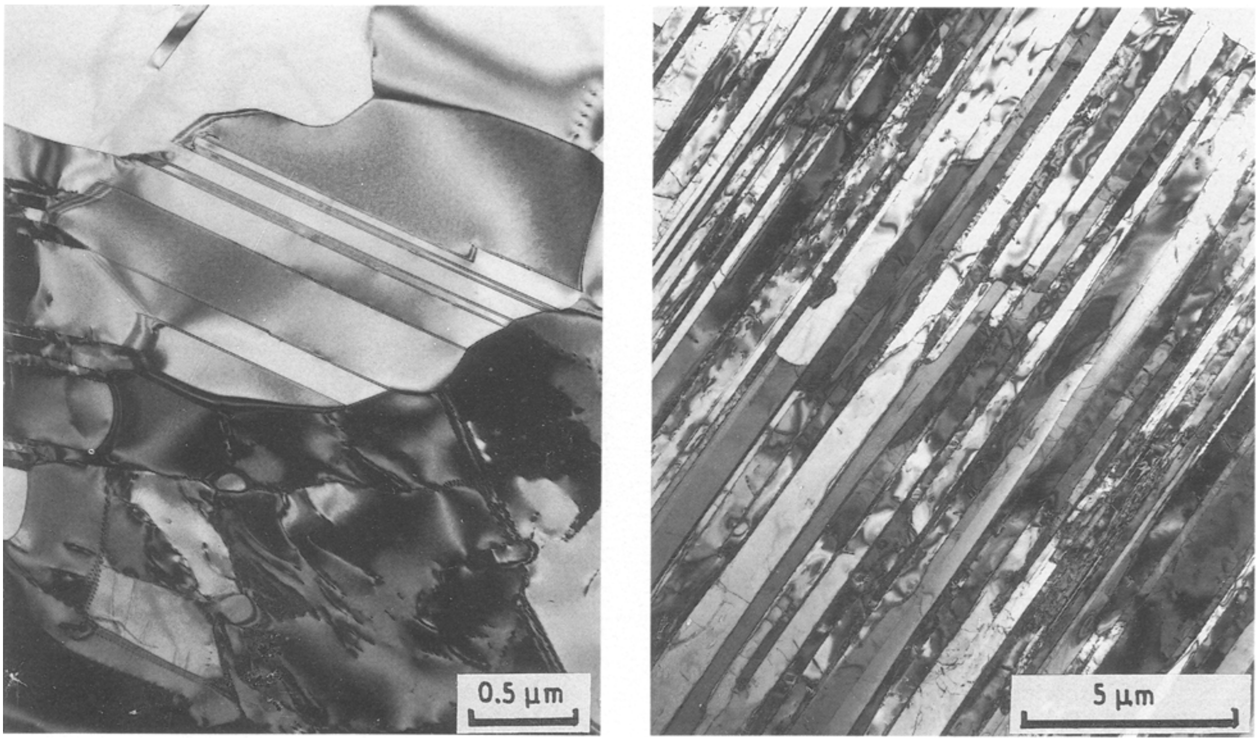

Figure 6 Variety of microstructures in γ-TiAl alloys (unpublished work by C. Suryanarayana at WPAFB, Ohio, 1990).

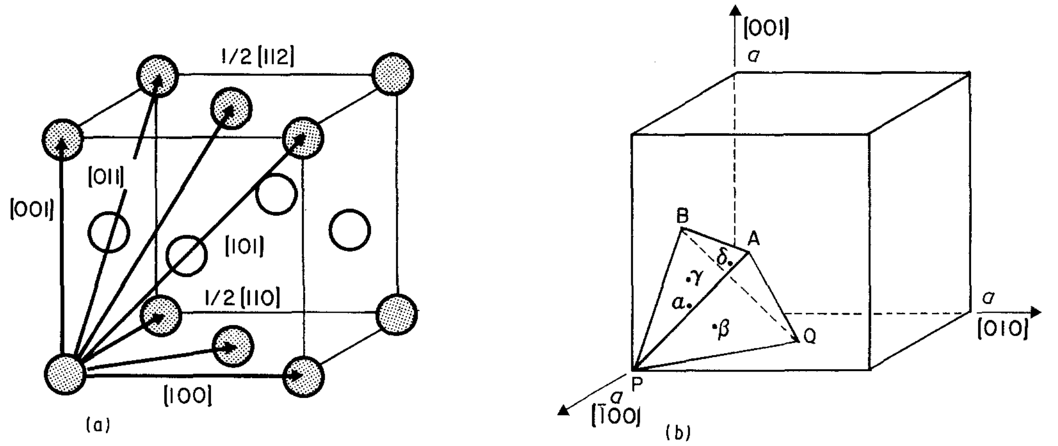

Figure 7 (a) Crystal structure and Burgers vectors in the TiAl (γ) phase and (b) modified Thompson tetrahedron for the $L1_0$ structure [140].

TABLE VI Magnitudes of the possible Burgers vectors in TiAl in ascending order; TiAl (with $c/a = 1.02$) is regarded as cubic (after [131, 134])

Thompson notation	Burgers vectors	Group notation	b^2
PQ	$\frac{1}{2}[1\,1\,0], \frac{1}{2}[1\,\bar{1}\,0]$	$\frac{1}{2}\langle 1\,0\,0]$	$\frac{1}{2}$
Pa[a]	$[1\,0\,0], [0\,1\,0], [0\,0\,1]$	$\langle 1\,0\,0]$	1
3Aβ, 3Bα	$\frac{1}{2}[1\,1\,2], \frac{1}{2}[1\,\bar{1}\,2], \frac{1}{2}[\bar{1}\,1\,2], \frac{1}{2}[1\,1\,\bar{2}]$	$\frac{1}{2}\langle 1\,1\,2]$	3/2
2PA, 2PB	$[1\,0\,1], [0\,1\,1], [1\,0\,\bar{1}], [0\,1\,\bar{1}]$	$\langle 1\,0\,1]$	2

[a] Not Thompson notation.

Thompson tetrahedron, modified for the $L1_0$ structure, can be used to describe the Burgers vectors and the dissociation reactions of the dislocations (Fig. 7b). In this diagram, A, B, P and Q are the vertices of the tetrahedron; α, β, γ and δ represent the centres of the faces opposite to the vertices A, B, P and Q, respectively. Any displacement vector connecting either A or B with P or Q leads to chemical disordering and therefore it is not likely that these dislocations will exist. Perfect dislocations are defined by two consecutive capital letters AB, PQ, etc; partial dislocations are described by mixed letters of one capital letter and one Greek letter, e.g. Pβ, βA, etc; and superdislocations are designated by mixed letter(s) and number (larger than unity), e.g. 2PB, 3βQ, etc. The Burgers vectors and magnitudes of the possible perfect dislocations in TiAl are presented in Table VI [131, 133, 134]. Movement of any of these dislocations does not destroy ordering.

On the basis of energetic considerations, $\frac{1}{2}\langle 1\,1\,0]$ $\{1\,1\,1\}$ is the most favourable slip system* and these dislocations have been observed in TiAl samples deformed at room temperature [128, 135–137] and higher temperatures [126, 127, 138–140]; these were, however, not observed in samples deformed at 77 K [130]. On the other hand $[0\,1\,1]$ and $[1\,0\,1]$ slip destroys the ordered structure and creates a series of complex faulted structures, implying that slip of these types may be feasible only if dislocations move in pairs so as not to disturb the ordered structure, i.e. superdislocations.

A variety of dislocation dissociations is possible and these produce complex stacking faults (CSF) and antiphase boundary (APB) structures. Some typical examples are as follows:

$$\tfrac{1}{2}[1\,1\,0] \rightarrow \tfrac{1}{6}[2\,1\,\bar{1}] + \text{CSF} + \tfrac{1}{6}[1\,2\,1] \qquad (1)$$

$$[1\,0\,0] \rightarrow \tfrac{1}{2}[1\,\bar{1}\,0] + \tfrac{1}{2}[1\,1\,0] \qquad (2)$$

and these can further dissociate according to Equation 1:

$$\tfrac{1}{2}[1\,1\,2] \rightarrow \tfrac{1}{6}[1\,1\,2] + \text{SISF} + \tfrac{1}{3}[1\,1\,2] \qquad (3a)$$

$$\tfrac{1}{2}[1\,1\,2] \rightarrow \tfrac{1}{6}[1\,1\,2] + \text{SESF} + \tfrac{1}{6}[1\,1\,2] + \text{SISF} + \tfrac{1}{6}[1\,1\,2] \qquad (3b)$$

$$[1\,0\,1] \rightarrow \tfrac{1}{6}[1\,\bar{1}\,2] + \text{SISF} + \tfrac{1}{6}[2\,1\,1] + \text{APB} + \tfrac{1}{6}[1\,\bar{1}\,2] + \text{CSF} + \tfrac{1}{6}[2\,1\,1] \qquad (4)$$

where SISF and SESF represent superlattice intrinsic and extrinsic stacking faults, respectively. A listing of all possible dissociations can be found elsewhere [130–132, 141].

The deformation modes in the TiAl-base alloys seem to depend on Al content (i.e. whether a small amount of α_2 phase is present or not) [136, 142], ternary alloying additions, temperature and purity [143–145]. The temperature dependence of deformation mode and dislocation structures have been reviewed by Whang and Hahn [131].

Only $\langle 0\,1\,1]$ and $\frac{1}{2}\langle 1\,1\,2]$ dislocations were observed in samples deformed at 77 K and $\frac{1}{2}\langle 1\,1\,0]$ dislocations were not seen [130], while all three types

---

* We will use the mixed notation $\langle h\,k\,l]$ to indicate a set of equivalent crystallographic directions which are generated by permutations of $\pm h$ and $\pm k$; only a sign change is allowed for l.

were observed on deforming the samples at room temperature [134]. Dissociation behaviour of these dislocations and formation of stacking faults and antiphase boundaries have been investigated by the weak-beam electron microscopy technique [134] because of the short fault widths. Although $\frac{1}{2}\langle 1\,1\,0]$ dislocations have been observed, they do not seem to dissociate into Shockley partials [128] as predicted by Greenberg [146]. Increasing the purity of the alloy appears to increase the density of $\frac{1}{2}\langle 1\,1\,0]$ dislocations [144] and the ductility [143].

Deformation of TiAl in the temperature range of room temperature to 600 °C (for single crystals and 800 °C for polycrystals) is accompanied by strain-hardening. Hence, the $\frac{1}{2}\langle 1\,1\,0]$ dislocations are curly and tangled due to massive cross-slip during deformation [127]. The $\langle 0\,1\,1]$ dislocations appear linear at 800 °C [126, 138] and dissociate into one superpartial and two Shockley partials and the APB lies on a $(1\,0\,0)$ plane, while the APB on room-temperature deformation lies on $(1\,1\,1)$; $\langle 1\,0\,1]$ dislocations and their dissociation have also been observed. Further $\langle 1\,0\,1]$ dislocations cross-slip on to other $\{1\,1\,1\}$ planes; evidence also exists that the APB between two superpartials lies on a $\{1\,0\,0\}$ plane instead of a $\{1\,1\,1\}$ plane [134].

At temperatures > 800 °C, TiAl and its alloys show a rapid decrease in strength, probably due to lattice softening and dislocation annihilation. The dislocation morphology at this stage is quite different; $\frac{1}{2}\langle 1\,1\,2]$ dislocations are long and stretched and the $\frac{1}{2}\langle 1\,1\,0]$ dislocations are not tangled or curled. Further, new $\langle 1\,0\,0]$ type dislocations also are activated [139]. These observations suggest that the positive temperature dependence of yield stress may be explained on the basis of either (a) $\frac{1}{2}\langle 1\,1\,0]$ $\{1\,1\,1\}$ slip dislocations becoming entangled at an intermediate temperature, or (b) a cross-slip model [134] involving $\langle 1\,0\,1]$ and $\frac{1}{2}\langle 1\,1\,2]$ dislocations, or (c) dislocation–dislocation pinning.

Twinning [147–149] has been found to help in increasing the ductility of TiAl alloys with $\{1\,1\,1\}$ $\langle 1\,1\,\bar{2}]$-type twins being most commonly observed. The tendency of increased twinning above the ductile–brittle transition temperature suggests that it is responsible for the increased ductility [142].

Fracture in these alloys is of the cleavage type, up to high temperatures. Slip dislocations move on $(\bar{1}\,1\,1)$ and $(1\,\bar{1}\,1)$ planes and meet along the $[1\,1\,0]$ direction. The leading superpartials are forced together by the stress concentration from the piled-up superpartials and change into the resultant dislocations. The second trailing superpartials on each slip plane are combined easily with the resultant dislocations. The combination of the resultant dislocations and the following piled-up dislocations results in wedge-shaped microcracks that connect and grow in the direction of the tension side, resulting in fracture [130, 141].

3.2.4. Mechanical properties

Alloys based on the TiAl (γ) composition have higher elastic modulus, lower density, enhanced elevated-temperature capabilities, and are less likely to ignite than Ti_3Al (α_2) alloys. However, room-temperature ductility and fracture resistance can only be classed as "poor" [83]. General trends are for a slight decrease in stoichiometry, into the two-phase $\gamma + \alpha_2$ region, to increase ductility [18], with small (1–3%) V, Mn and Cr additions enhancing ductility [20, 28, 30–33, 119–121], or Nb, Ta and Mn improving stength and oxidation resistance [122, 123, 150]. The interested reader is referred to comprehensive papers by Kim [30, 33] for more details on factors controlling ductility in γ-based alloys. As with the α_2 alloys, thermomechanical processing allowing production of a range of microstructures also strongly influences mechanical properties [30–33]. The Ti–52Al alloy demonstrates the lowest hardness value at room temperature independent of the TMP treatment [151–154]. At 1000 °C, however, the strength tends to gradually decrease with increasing Al level [30–33]. Tensile strength and hardness vary in the same fashion with changes in aluminium content [30–33]. The room-temperature (RT) tensile elongation is maximum at approximately Ti–48Al. Values of room-temperature ductility slightly in excess of 2% elongation are possible with chemistry control (two-phase region) and microstructure (combined lamellar/equiaxed) [33, 124], although an excursion down to the nanostructure region of microstructure scale can apparently increase this level up to 5%, and at the same time decrease the ductile-to-brittle transition temperature by as much as 200 °C [125].

Low-cycle fatigue experiments [29] suggest that fine grain sizes raise the fatigue life at temperatures below 800 °C. Fatigue crack growth rates are more rapid than those for superalloys, even when density-normalized [93]. Both fracture toughness and impact resistance are low at ambient temperatures, but fracture toughness increases with temperature [29]. Fracture toughness increases with higher proportions of the lamellar structure [33]. In a two-phase quaternary γ alloy a fracture toughness of $12\ \mathrm{MPa\,m^{1/2}}$ is observed for a fine structure which is almost entirely γ, and $K_{\mathrm{Ic}} > 20\ \mathrm{MPa\,m^{1/2}}$ when a large volume fraction of lamellar grains are present [30–33].

Creep properties are improved beyond the behaviour of superalloys when normalized by density, but are strongly influenced by alloy chemistry and TMP. For example, increased Al content and additions of W [154] or C [29] increase creep resistance. In the single-phase γ region (Ti–53.4Al) there was no influence of grain morphology on creep behaviour [155]. However, at leaner Al contents (Ti–50Al) a small amount of second phase was observed along with enhanced creep behaviour and a clear improvement in creep behaviour with increasing grain size [156]. This latter work suggested that creep in TiAl is not simply diffusion-controlled as it is in normal metals. Increasing the volume fraction of the lamellar structure enhances creep properties [29, 33], but lowers ductility. The level of creep strain occurring due to elongation on initial loading and primary creep is a concern since it can exceed projected design levels for maximum creep strain in the part [83].

4. Processing techniques

4.1. Ingot and casting

Melting, solidification and processing of the α_2 compositions, while not easy, are an extension of the melting parameters used for conventional terminal titanium alloys [157–159]. However, the extremely low ductility of γ compositions has necessitated the use of innovative practices including much smaller than normal ingots for the γ compositions (200 kg [159]) and the exercise of great care in cooling of the ingots to avoid cracking due to thermal stresses. Subsequent processing of γ ingots to various mill product forms has been carried out with a great deal of caution: higher temperatures, smaller reductions, and increased conditioning compared to conventional alloys.

Near net shape (NNS) cast components are particularly attractive for titanium aluminides, especially the γ-compositions, since difficult working operations are eliminated. For the α_2 composition casting parameters are close to those for the Ti–6Al–4V alloy, despite some flow problems [158]. The use of the TCP method (see below) will allow refinement of the microstructure of the α_2 composition at least, but no reported studies have yet been carried out in this area.

A fruitful area for further study is the use of small additions of yttrium or other rare-earth elements to enhance the workability and ductility of both the α_2 and γ titanium aluminides [160–162]. Small amounts of Y for example (< 100 p.p.m.), added in a highly controlled fashion, should lead to numerous advantages including increased metal yield, reduced cost, improved inspectability, and overall mechanical behaviour enhancement [163].

4.2. Powder metallurgy

The powder metallurgy (PM) approach is used in general terms to either reduce cost or enhance behaviour [163, 164]; and well established, cost-effective techniques which have been developed for the production of NNS conventional titanium alloys, such as Ti–6Al–4V, are readily adapted for use with both families of aluminides [165]. Techniques which allow improved properties such as rapid solidification [164, 166–169] and mechanical alloying [170–172] can also be used with the titanium aluminides. Additionally, a number of other PM methods such as reactive processing [173] have been applied to these alloys.

4.2.1. Conventional PM

Because of the extreme difficulty in fabricating the γ compositions Schafrik [174] used a blended elemental (BE) approach followed by extrusion to bar product. Further optimization is required with consideration given to homogeneity, the effect of remnant chloride/voids, and the various phases which have been detected [175].

Early work using γ compositions and pre-alloyed (PA) powders was partially successful [176, 177] with problems due to porosity, coarse grains and cracks. More recently parts from both families of titanium aluminides have been produced utilizing the plasma rotating electrode process (PREP) [178] and gas atomization (GA) [179, 180] methods (Fig. 8a and b [180]). The mechanical properties of compacts were equivalent to those attained by ingot techniques.

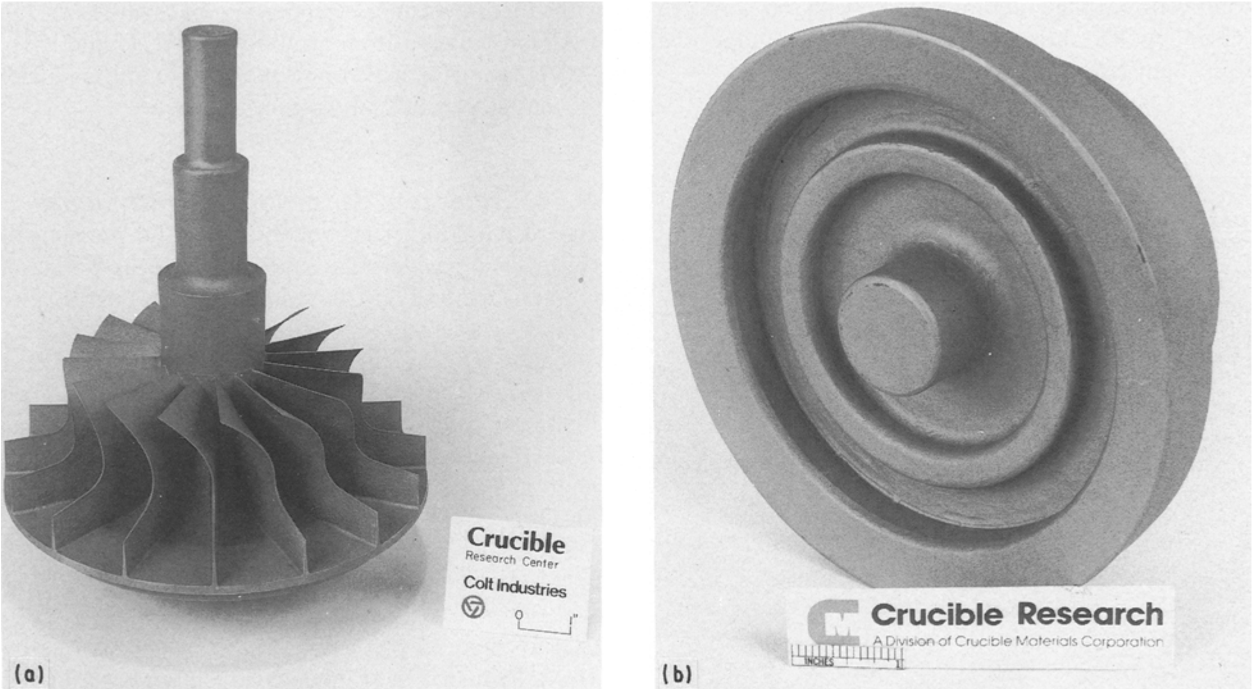

Figure 8 (a) Turbine engine compressor rotor produced by HIP of α_2 PREP powder and (b) machining preform produced by HIP of gas-atomized γ powder using the ceramic mould process [180].

4.2.2. Rapid solidification

Rapid solidification (RS) processing of the titanium aluminides offers the potential of improved ductility by disordering, grain refinement, and deoxidation of the matrix, and enhanced elevated-temperature properties due to a dispersion of fine, thermodynamically stable second-phase particles [166–169, 181–188].

4.2.2.1. α_2 alloys. Rapid solidification of Ti_3Al–Nb alloys with rare-earth additions such as Er result in a refinement in the grain size and a dispersion of Er_2O_3 particles (Fig. 9) [70, 189–196]. Some increases in room-temperature ductility and elevated-temperature performance occur [197–199]. However, in general it must be concluded that in comparison with aluminium alloys in which a dispersion of as much as 25–30 vol % can be obtained [200–202], with resulting significantly enhanced elevated-temperature performance, the 1–3 vol % rare-earth oxide obtained in RS Ti_3Al alloys (and Ti-based alloys in general) is quite disappointing.

4.2.2.2. γ alloys. The γ phase forms by a peritectic reaction, therefore RS can lead to a large improvement in alloy homogeneity and formation of metastable phases and microstructures. RS TiAl alloys often contain metastable α_2, and evidence of metastable disordered TiAl has been observed [203–210]. Studies of the solidification of RS Ti–50 Al powder indicated some dendrites with sixfold symmetry [208] that was initially thought to be due to undercooling of the melt; however, this has now been shown to be the equilibrium solidification path for some TiAl alloys.

The homogeneous and fine microstructure of RS alloys [67] leads to improvements in the ductility of γ alloys at room temperature. Further, alloys in the composition range of approximately 48–60% Al processed by RS showed a consistent advantage over equivalent IM material [211, 212].

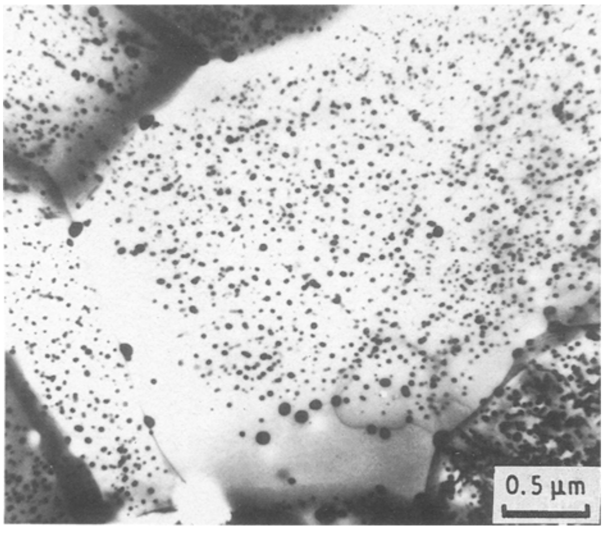

Figure 9 Er_2O_3 dispersion in a rapidly solidified Ti_3Al–2 wt % Er alloy HIPed at 850 °C [196].

Ternary additions of Co, Cr, Fe, Ge, Mn, Ni, V and W have been made to RS TiAl-based alloys [204, 213]. Co, Fe, Ni and W additions result in the greatest hardening observed in TiAl alloys, and additions of Cr, Mn, and V have been reported to improve the room-temperature ductility of RS Ti–48% Al alloys [213] to 3.5%, up from $< 1\%$ in the binary alloy.

Thus it appears that, in combination with the near-net-shape advantages offered by PM fabrication, RS may offer some advantages for the processing of γ alloys over the ingot approach; presently the same cannot be said for RS processing of α_2 alloys.

4.2.3. Mechanical alloying

The mechanical alloying (MA) powder metallurgy approach allows even further departures from equilibrium than RS [3, 4, 6–8, 11, 13, 16, 170], and thus increased opportunities to produce novel microstructures, and in turn enhanced mechanical properties. Little work has been done on MA of the titanium aluminides, but that reported suggests that this may be an interesting fabrication method for both the α_2 and γ families of alloys [171, 172]. MA of a number of α_2 alloys including Ti–24Al–11Nb and Ti–25Al–10Nb–3V–1Mo, with and without rare-earth additions, resulted in a refinement in grain size, especially when a large amount of the B2 phase was present (Ti–25Al–10Nb–3V–1Mo), which persisted even after exposure at 1090 °C for 6 h. Further, little dispersoid coarsening occurred, and there were no dispersoid-free zones close to grain boundaries as observed in RS alloys [172]. However, MA conditions were clearly not optimum in this work, with mixed grain sizes and relatively coarse rare-earth oxide particles, and further studies are necessary.

Mechanical alloying has been used in conjunction with thermochemical processing to synthesize the TiAl composition from a mixture of Al_3Ti and TiH_2 [214]. Again, further work is required to fully evaluate the viability of this fabrication technique.

4.2.4. Other powder metallurgy techniques

The reaction sintering and hot isostatic pressing of pre-reacted powders have been studied as potential synthesis methods for TiAl starting from blended elemental powders [173]. While the reaction sintering was unsuccessful, the pre-reacted approach gave a fully homogeneous TiAl matrix, with a dispersion of alumina particles, and properties at least as good as those obtained from a pre-alloyed approach. This could well lead to a reduced-cost PM processing route for TiAl.

4.3. Thermochemical processing

Thermochemical processing (TCP) is a technique by which hydrogen is added as a temporary alloying element to titanium-based materials to enhance processability and refine the final microstructure; the latter characteristic leads to significantly improved mechanical properties, particularly those which are crack initiation-related such as fatigue [215, 216]. It is very attractive for refinement of the microstructure with near-net-shape (NNS) fabrication methods, such as castings or powder metallurgy, where the working operation normally used to reduce the scale of the microstructure in wrought product cannot be used.

Preliminary studies on the applicability of TCP to the α_2 alloy Ti–24Al–11Nb demonstrated that plasma rotating electrode process (PREP) powder could be successfully compacted by hot isostatically pressing (HIPing) at $\geqslant 100\,°C$, lower temperatures with hydrogen-containing powder than with normal powder [217, 218]. Additionally, a significantly refined microstructure was obtained. Full evaluation of the advantages to be gained with TCP of the α_2-type alloys remains to be studied; however, the TCP technique is being used on a semi-commercial basis in the Soviet Union to process α_2 and other difficult-to-fabricate titanium alloys [219].

The face-centred tetragonal γ ($L1_0$ structure) has virtually no solubility for hydrogen under generally applied temperatures and pressures [215, 216]. However, stabilization of the α_2 phase using RS [208] can allow hydrogen to enter the structure of a nominal TiAl composition [220], thus opening up the possibility of using TCP with this composition. Preliminary work has also demonstrated that hydrogen can be used to assist in the formation of TiAl by mechanical alloying [214]. Clearly much further work is required to define the potential of TCP with the γ-type alloys.

4.4. Designer microstructures

One method of improving the "forgiveness" of ceramic materials is by dispersion of a ductile phase in the brittle ceramic matrix [221–223]. This concept has recently been applied to the γ titanium aluminides by blending Ti–36Al PREP powder with either powders of commercially pure titanium or Ti–50Nb [224]. No improvement in compressive strain or toughness was recorded, perhaps because of microporosity, but metallographic work indicated that the second-phase ductile particles arrested cracks propagating through the γ matrix. Other work using Ti–6Al–4V, a β titanium alloy, or a niobium-based alloy [225, 226] powder at the 10–20 vol % level in a γ matrix resulted in increased toughness when excessive reaction between the ductile phase and the matrix was minimized [227, 228], a Ti–30Nb ductile phase working very well [225, 226]. Clearly this is a fruitful area for further exploration, with developments in the ceramics area serving as useful guidelines to follow.

5. Composite concepts

5.1. Concept

In a composite concept a second phase, which can have a particulate, short-fibre, continuous-fibre, or lamellar-type configuration [229] is introduced into the matrix to enhance physical and mechanical behaviour. Generally, the type of reinforcement which has been used with the intermetallic titanium aluminides has been continuous fibres, although considerable attention has been given to a novel *in-situ* concept. The major attributes of the continuous-fibre approach are that elevated-temperature strength and stiffness are enhanced, and at the same time the fibres can provide increased toughness by at least three mechanisms [229], all of which involve additional work:

(i) plastic deformation of the matrix,
(ii) fibre pull-out, and
(iii) presence of weak interfaces/fibre separation, and deflection of the crack.

This latter attribute of the MMC approach could well play a major role in the application of titanium aluminides using "damage tolerant" designs in which fracture toughness and fatigue crack growth rate are more important than ductility [230]; some cast superalloys in service have ductility levels of less than 2% at room temperature [230].

5.2. Continuous fibres

The advantages to be gained by embedding ceramic fibres in a titanium matrix have received considerable attention [231–237]. The enhancement in longitudinal tensile strength which is theoretically predicted from rule-of-mixtures (ROM) calculations, and has actually been achieved over a substantial temperature regime,

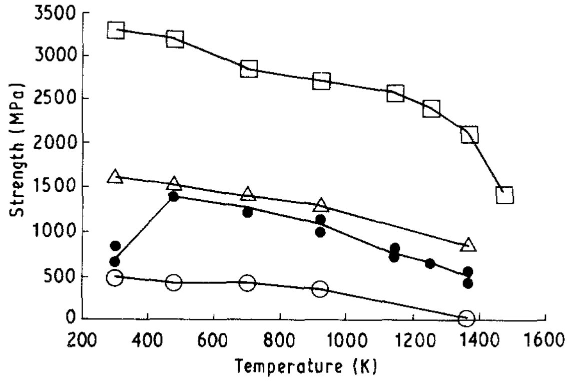

Figure 10 Tensile strength versus temperature for (☐) SiC fibre (0.014 cm), (○) Ti_3Al + Nb, (●) SiC/Ti_3Al + Nb (40 vol % fibre), and (△) ROM prediction (40 vol % fibre) [238].

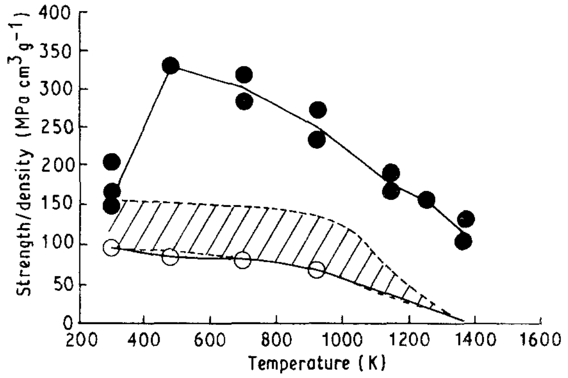

Figure 11 Comparison of σ/ρ values of (●) SiC/Ti_3Al + Nb (40 vol % SiC), (○) Ti_3Al + Nb and (shaded) wrought René 41 and Hastelloy X superalloys for a range of temperatures [238].

is shown in Fig. 10 [238] with the actual values averaging about 77% of the ROM predicted values. A density-normalized plot of the SiC/Ti_3Al + Nb data versus wrought superalloy data (René 41 and Hastelloy X) indicating the attraction of the intermetallic system is shown in Fig. 11 [238].

5.2.1. Fibre compatibility and availability

The desirable characteristics of a reinforcing fibre are [239, 240]

(i) compatible coefficient of thermal expansion (CTE) with the matrix,

(ii) chemical compatibility with the matrix even after extended elevated-temperature exposures,

(iii) low density,

(iv) high modulus of elasticity,

(v) high strength at elevated temperature,

(vi) good oxidation resistance,

(vii) 50–250 μm diameter continuous monofilament, and

(viii) mass-production feasibility (including affordable cost).

The first two items depend on the behaviour of both the fibre and the matrix, whereas the latter six of these characteristics are attributes of the fibre itself. Silicon carbide fibres with the required last six characteristics are currently available, and a number of other fibres (such as Al_2O_3) are in various stages of development [229, 239]. However, the compatibility issues of CTE mismatch and chemical interaction are not yet resolved.

Measured CTE values for two fibres, SiC (SCS-6) and Al_2O_3, and two representative matrices (α_2 and γ) are shown in Fig. 12 [241]. The CTE for the aluminides is more than twice that of the SCS-6 fibre, while the CTE of the Al_2O_3 fibre more closely approaches that of the potential matrix materials. This CTE difference means that upon cool-down after consolidation significant stresses occur [242, 243] which can degrade behaviour.

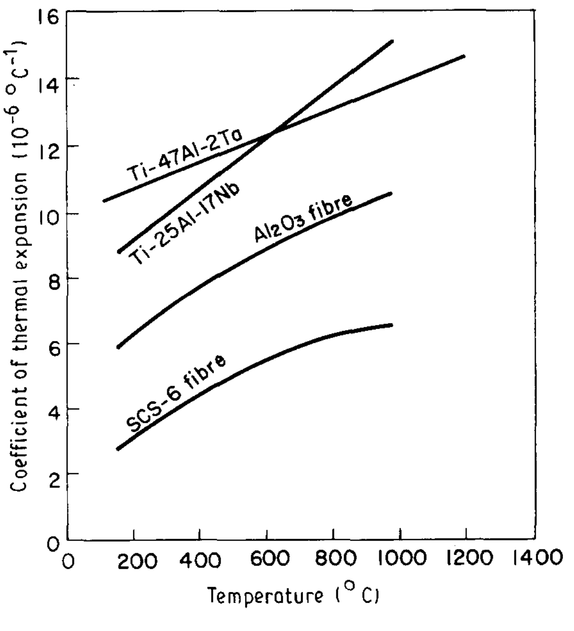

Figure 12 Coefficients of thermal expansion of fibre reinforcements and titanium aluminide matrix alloys determined at various temperatures by thermomechanical analysis [241].

Chemical reaction between the fibre and the matrix may be the major reason for less than ROM for many of the mechanical properties in titanium matrix composites [232, 233, 238, 241, 244–259] (Fig. 13 [252]), with increasing thickness of the complex reaction zone being related to a general degradation in mechanical properties [260, 261]. This relationship has spawned a considerable amount of work on fundamental thermodynamic studies of chemical compatibility using phase diagrams [253, 254, 262] where minimal reaction of the titanium aluminides with Al_2O_3, TiB_2, CaO, Ti_5Si_3, Y_2O_3, rare-earth oxides and sulphides, and TiN has been reported. Factors such as trace elements and crystal structure clearly play a role in explaining discrepancies between various studies.

In studies of actual titanium-matrix fibre composites it is clear that less reaction takes place between fibres such as SCS-6 and Ti_3Al than with the conventional alloy Ti–6Al–4V [231–234, 238, 250]; and that with increasing Nb addition to the Ti_3Al the reaction zone width decreases [246]. Considerable reaction also occurs between TiAl and SCS-6 [241, 244, 250], particularly, with the higher fabrication temperature used with this alloy. No reaction was reported between Al_2O_3 fibres and a Ti–45Al–2Ta (γ) matrix which in combination with the lower CTE mismatch makes this an interesting system [241]; surface flaws on the Al_2O_3 may necessitate a coating for mechanical compatibility with the matrix [241].

Comprehensive studies using fibre push-out techniques [94, 261] indicate that the room-temperature chemical bonding (119 MPa shear stress) is more than twice as high as the frictional bonding due to CTE differences (48 MPa) in a Ti–24Al–11Nb/SCS-6 composite; no significant reduction in strength was noted, with debonding occurring at the remaining coating–reaction-zone interface.

The major problem with fibre–matrix incompatibility is illustrated under conditions of purely thermal fatigue, which led to residual stresses from moduli and CTE mismatches and extensive matrix damage in a Ti–24Al–11Nb/SCS-6 composite (Fig. 14 [263]). Clearly with the brittle matrices involved not only is a diffusion barrier necessary to limit interfacial chemical reactions, but also compliant layer coatings to accommodate CTE differences.

Based on thermodynamic data, coatings of TiC, TiB_2 and CaO were applied to Sigma SiC and α-Al_2O_3 fibres prior to insertion into a γ (Ti–47Al–2Ta) matrix [253]. Little or no reaction with TiB_2, CaO or straight Al_2O_3 was noted. However, TiC was found to react with the SiC. A study of Pt + W coating on SCS-6 fibres in a γ (Ti–48Al–1V) matrix indicated virtually no reaction, suggesting that this combination may help to solve both the CTE and reactivity problems [256]. Many other coatings are possible [262, 264]; however, the ultimate test will be to investigate thermal cycle effects and the mechanical properties of the composite [253]. Another, but perhaps even more challenging solution is to develop

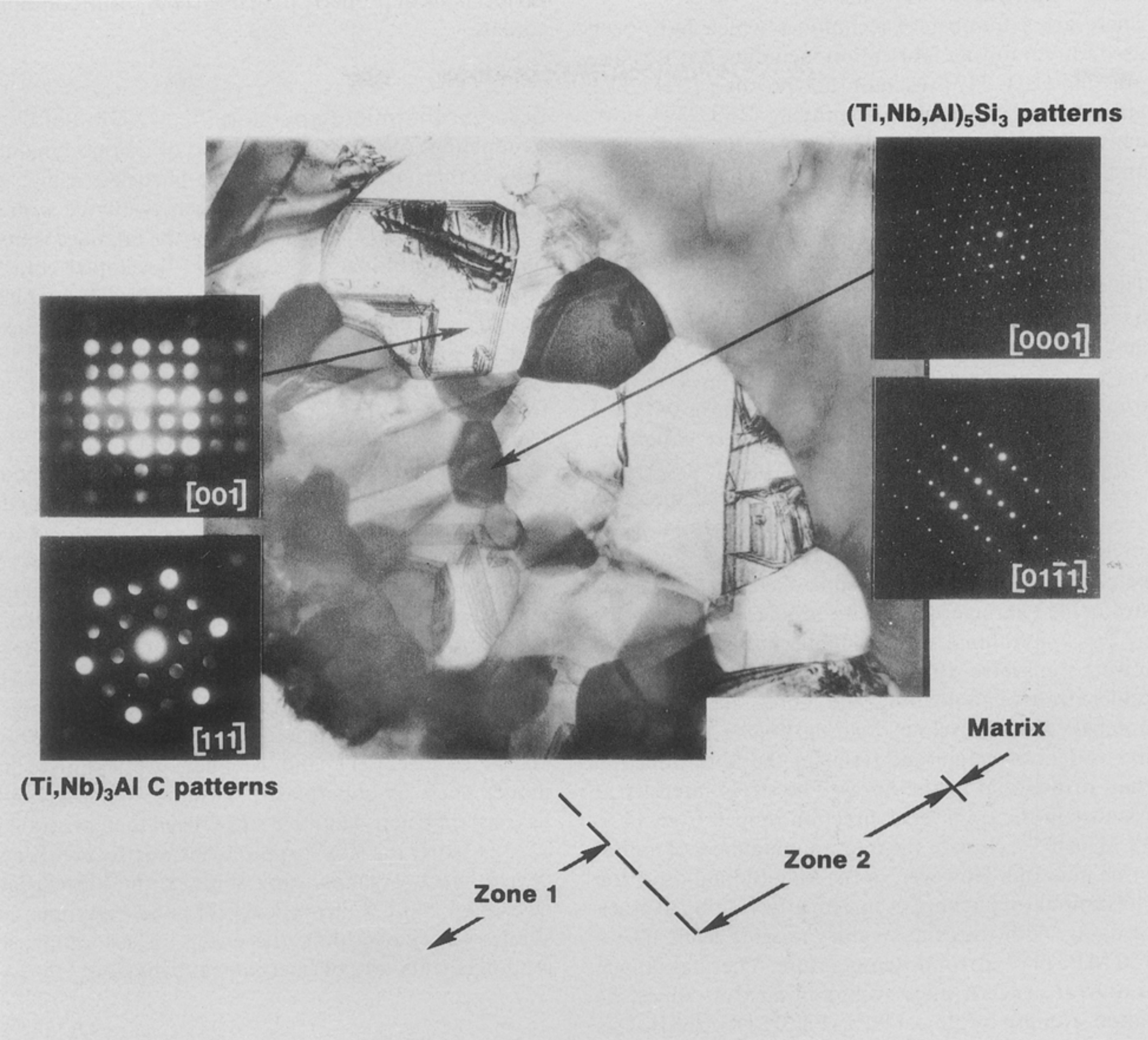

Figure 13 High-magnification micrograph of the reaction zone. Diffraction patterns on left are from the (Ti, Nb)$_3$AlC phase, which are seen as faulted grains in the micrograph. Patterns on the right are from the (Ti, Nb, Al)$_5$Si$_3$ particles, one of which is indicated with an arrow [252].

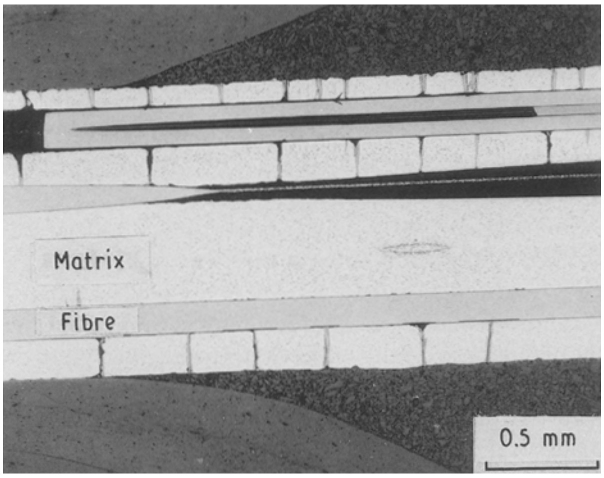

Figure 14 Internal transverse matrix cracking in a Ti–24Al–11Nb/SCS-6 composite experiencing 500 cycles in the temperature range of 150 to 815 °C [263].

a more "forgiving" matrix (composition and/or microstructure) while maintaining good elevated-temperature properties; it could well be that the high fracture toughness α_2 alloy (42.3 MPa m$^{1/2}$, Table V [86, 91]) could be optimized as a matrix for "forgiveness" and environmental resistance, letting the fibres bear the stresses – the concept used in polymeric matrix composites [229].

At the present time there is only one fully commercial source of SiC fibre partially optimized for use in a titanium matrix – the 150 μm SCS-6 fibre which is produced by chemical vapour deposition (CVD) with a coating of carbon-rich non-stoichiometric amorphous SiC on top of amorphous carbon, with a total coating thickness of about 2.5 μm [235–237, 239]. This coating blunts the intrinsic surface flaws resulting from CVD, and greatly reduces the chemical interaction between the fibre and the matrix. A second 100 μm SiC-based fibre is rapidly approaching commercial production status [237], with three alternate surfaces being offered: uncoated, structured-carbon coated and titanium diboride coated. Other fibres such as B$_4$C/B, Borsic and B-fibres appear unsatisfactory for use in a titanium matrix [231, 233]. However, another alternative which is also being evaluated is Al$_2$O$_3$ fibres [265].

5.2.2. *Composite fabrication*

There are a number of techniques which have been used for composite fabrication including hot isostatic pressing [231–237], vacuum hot-pressing [231–237], arc-spraying [239], plasma spraying [180, 239], powder cloth technique [238, 239], woven fibre mat [83], and electron-beam vapour deposition [266].

5.2.3. *Mechanical properties*

The mechanical properties of SCS-6/(Ti–24Al–11Nb) have recently been reviewed in detail [83]. Longitudinal strengths are generally close to ROM values with the behaviour being controlled by the fibres, but the transverse properties are significantly lower with the strength being controlled by the matrix capability [267, 268]; there is creep-mirrored tensile behaviour with the rupture stress in the longitudinal direction being an order of magnitude better than at right angles to the fibre direction. Fatigue crack initiation behaviour appeared to be controlled by the matrix strain–life characteristics, with notches degrading life in the longitudinal direction but not in the (much lower) transverse direction [268]. This suggests that under transverse loading the fibres act as potent notches. Under cycling, loading cracks propagated five orders of magnitude faster in the fibre direction than orthogonal to the fibres. The stress intensity at fracture in the transverse direction ranged from 14 to 19 MPa $m^{1/2}$, close to the fracture toughness of monolithic material. However, in the longitudinal direction substantial toughening occurred, attributable to crack bridging, with toughness values ranging from 110 to 150 MPa $m^{1/2}$ at room temperature. Thermal fatigue is a great concern since cycling in air can reduce the initial strength by almost 90% (Fig. 15 [83, 263]). This degradation has been attributed to heavily oxidized surface cracks [269], which do not occur in vacuum [270]. Thus, while the composite α_2 material does demonstrate enhanced behaviour in some areas, several concerns remain including transverse properties, environmental resistance and designing with a material of limited ductility.

The even lower inherent "forgiveness" of the γ compositions has precluded the development of meaningful mechanical property data from composite concepts to date.

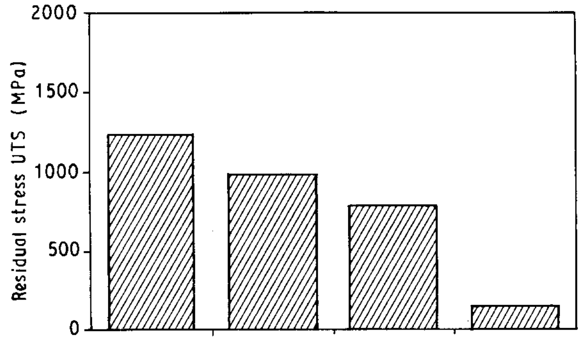

Figure 15 Longitudinal tensile strength of unidirectional SCS-6/Ti–24Al–11Nb composite versus number of prior 150 to 815 °C thermal cycles in air [83].

5.3. Exothermic dispersion

Production of XD^{TM}, a dispersion of thermodynamically stable *in situ* second-phase particles, using an exothermic reaction [271], has been evaluated with a γ-matrix [272–277]. In this process the interface is free of reaction products or externally developed contamination such as an oxide layer [273, 277] which should avoid easy decohesion of the reinforcing phase, and early failure [273]. The microstructure of XD^{TM} γ containing the TiB_2 phase can be controlled both in terms of matrix grain size [275] and morphology (lamellar or equiaxed) [274], and the shape of the reinforcing particles [273, 274], resulting in material with enhanced room-temperature and elevated-temperature strength [271, 273]. The best room-temperature ductility is obtained from an equiaxed matrix morphology in combination with particulate reinforcement ($\sim$ 1% elongation), while a lamellar–short fibre combination optimizes strength, creep resistance and fracture toughness (17 MPa $m^{1/2}$) [274]. Various mill products are available including forgings, extrusions, investment casting, powder metallurgy and rolled sheet [271] and secondary fabrication techniques such as superplastic forming, welding, and brazing/diffusion bonding have been demonstrated [271]. Clearly the XD^{TM} approach is worthy of further development, perhaps using some of the knowledge developed in other theoretical [278] and experimental studies [279] regarding the effects of second-phase reinforcements in γ on mechanical behaviour.

6. Environmental effects

The inherently attractive elevated-temperature characteristics of the titanium aluminides imply that in use these materials will often be exposed to hostile high-temperature environments, which can be hot air at high pressure in engines [280, 281], or hydrogen ranging all the way from cryogenic liquid hydrogen to elevated-temperature high-pressure gaseous hydrogen in components of the National Aerospace Plane (NASP) [282, 283].

6.1. Oxygen-rich environments

6.1.1. *Background*

Oxidation studies of titanium and titanium alloys in the temperature range 400–700 °C indicated that on exposure to air a complex oxide scale is produced whose structure is laminated and composed of several oxides ranging between TiO and rutile TiO_2 [37, 284–292]. The oxidation resistance of Ti does not improve appreciably for Al concentrations up to about 13Al [293–295], but with increasing Al above this level the oxidation rate is reduced [293, 296].

6.1.2. *Ti_3Al (α_2)*

The oxidation behaviour of Ti_3Al alloys at 760 mm

Hg oxygen pressure in the temperature range 700–900 °C [37] is better than that of the conventional high-temperature titanium alloy IMI 834. Higher niobium concentrations improve the oxidation resistance, with Ti_3Al + 11Nb running out of oxidation resistance at 800 °C. In general, it appears that Ti_3Al alloys follow mixed kinetics, resulting from the combined oxidation of titanium and aluminium, with the formation of three zones in the oxide layer. The top, relatively loose cracked layer contains mostly rutile (TiO_2) and a small amount of α-alumina. The middle layer is again a mixture of titania and alumina, with a high titania/alumina ratio, and the bottom layer is mostly metallic, being a depleted zone and most probably not ordered like Ti_3Al.

A study of the oxidation behaviour of titanium aluminides (Ti–36Al, Ti–34Al) in the temperature range 600 to 1100 °C indicated that the scale consists of alternate layers of TiO_2 and Al_2O_3-rich oxides [297]. At high oxidation temperatures the oxidation kinetics tend to be dominated by TiO_2 formation, while at lower temperatures more aluminium is present, and an adherent alumina scale forms. This restricts inward oxygen diffusion and limits embrittlement.

In section 5.2.1 it was noted that the combination of residual stresses in the matrix and a brittle oxide layer could result in transverse matrix cracking purely from thermal cycling in air in Ti–24Al–11Nb/SCS-6 composites [262]. This leads to a reduction in longitudinal tensile strength by almost 90% after 500 thermal cycles. The large adverse effect of the oxygen is demonstrated from testing of vacuum-encapsulated samples where no such severe degradation is recorded [83, 263]. This detrimental effect of oxygen is also found in tensile [298], creep [270] and fatigue crack growth [299] studies, with early crack initiation being attributed to brittle α-case.

6.1.3. *TiAl (γ)*

TiAl has a poor resistance to oxidation at temperatures above about 800 °C, because the external layer of the oxide is not a protective Al_2O_3 film, but TiO_2 or a mixture of TiO_2 and Al_2O_3 [289, 300]. Alumina scale can form on TiAl initially but it does not act as a protective film because of the high diffusivity of titanium in the Al_2O_3 scale, which produces crystalline TiO_2 as an external scale. The crystal growth of randomly oriented grains of TiO_2 leads to the formation of numerous voids and pores at the grain boundaries which trigger crack initiation and spallation of oxide films from the alloy substrate. The spallation of the crystalline TiO_2 layer is enhanced by thermal cycling, resulting in an acceleration of oxidation. Surface condition can strongly influence the oxidation scale formed, with a ground surface resulting in a more adherent alumina scale than an electropolished surface [297].

6.2. Hydrogen-rich environments

6.2.1. *Background*

Hydrogen can strongly adversely effect the mechanical properties of titanium (or other) based materials by reducing strain to failure, causing a brittle intergranular failure mode. When hydrogen originates from an external source the microstructure can have a large effect on behaviour. Fracture has been related primarily to hydride formation, which occurs with a 23% volume increase, but can also occur at α–β interfaces. Since hydrogen embrittlement depends on the attainment of a critical hydrogen chemical potential at points of stress concentration, alloys with lower solubility are less likely to suffer adverse consequences from the hydrogen environment than those with high solubility (Fig. 16 [215, 216]). Thus, the terminal alloy Ti–6Al–4V is more susceptible than the α_2 class of aluminides, and the γ class of aluminides is likely to be immune to hydrogen under normally applied pressures.

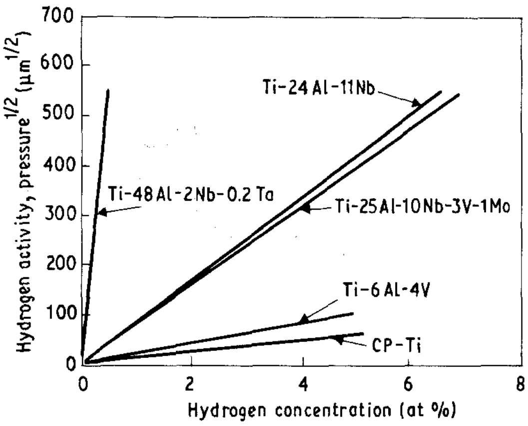

Figure 16 Hydrogen activity for selected titanium alloys at 800 °C [215, 216].

6.2.2. *Ti_3Al (α_2)*

Determination of the hydrogen susceptibility of α_2 indicates that hydride formation occurs in both Ti_3Al and Ti–Al–Nb [301]. Thin plates 80 nm wide with a $\{10\bar{1}0\}$ habit have been reported, with the hydrides dissociating at 700 °C. Embrittlement due to hydrogen gas has been reported for both Ti–24Al–11Nb and Ti–25Al–10Nb–3V–1Mo [302–304]. Severe embrittlement in 34.5 MPa hydrogen was noted at room temperature and at 204 °C with the crack path following the α_2–β interface. Ti–25Al–10Nb–3V–1Mo cracks after exposure to hydrogen at temperatures as low as 510 °C [305].

Almost all hydrogen in a precharged α_2 exists as hydrides because the terminal solubility of hydrogen in this alloy is very low at room temperature. Chu *et al.* [306] showed that in a Ti–24Al–11Nb alloy the cleavage cracks in a bluntly-notched bend bar (with or without hydride) nucleated adjacent to the notch root, and suggested that the cleavage-like cracking in this alloy is not controlled by normal stress alone but has some dependence on the applied strain. Strength increased and ductility and fracture toughness decreased with increasing amounts of hydrides. These parameters also changed significantly above a critical strain rate, with the critical value decreasing when hydrides were present. Gao *et al.* [307] detected a high volume fraction of titanium hydrides in Ti–24Al–11Nb alloys thermally charged in hydrogen at 1 atm for 6 h at 500 °C and cooled to room temperature.

Hydrogen-induced cracking and hydride formation in front of the crack tip and ductility loss have been reported for both Ti–24Al–11Nb and Ti–25Al–10Nb–3V–1Mo by Eliezer and co-workers [308–310]. The α_2 is very susceptible to hydrogen embrittlement, probably due to either some form of lattice bond interactions or the result of localized, strain-induced hydride formation in front of the crack tip, which decomposes after fracture.

Little information is presently available relative to the influence of hydrogen on fibre-reinforced metal-matrix composites. Areas of concern are the potential for accelerated hydrogen transport along the fibre–matrix interface and the increased ease of molecular hydrogen precipitation at the weaker and readily available fibre–matrix interface. Both graphite and SiC fibres may be significantly degraded by the presence of hydrogen at high concentrations in the host metal matrix [311].

6.2.3. TiAl (γ)

Hydride formation has not been detected in TiAl exposed to high-pressure hydrogen (13.6 MPa) at temperatures to 982 °C [305] and detailed fractographic analysis indicated that there is no effect due to 13.8 MPa hydrogen from − 130 °C to 204 °C [312]. A reduction in tensile strength in the near-γ alloy Ti–48Al–2.5Nb–0.3Ta occurred in hydrogen gas at room temperature after pre-exposure to hydrogen at 13.6 MPa and 815 °C for 30 min [313]. Matejczyk and Rhodes [314] investigated the effect of 12.8 MPa hydrogen charging at 650 °C for 100 h on the microstructure of Ti–48.6Al–2.4Cr (a two-phase alloy with $< 5\%\ \alpha_2$) and found the presence of a hexagonal phase, enriched in hydrogen, which has a volume contraction of 7% relative to the γ-TiAl matrix. This hexagonal phase has also been observed in Ti–48Al–1V alloy similarly exposed to high-pressure hydrogen [272].

High-temperature hydrogen exposure has no effect on the fracture toughness of Ti–45Al–3V with 7.5 vol % of dispersed TiB_2 phase, regardless of the prior microstructure state [315].

7. Commercialization

It can take 30 years or more from the research stage to get a new material into full-scale use in demanding flying applications [316–319]; and this is with "forgiving" materials. With "non-forgiving" materials such as the monolithic and composite titanium aluminides the time period for commercialization will clearly be extended further, even with creative design philosophies which emphasize toughness rather than ductility, use anisotropic behaviour to advantage, and use a concurrent engineering approach. Further, with the high initial cost of most emerging new materials the total cost, that is the acquisition and ownership cost, must be used as the criterion for material selection.

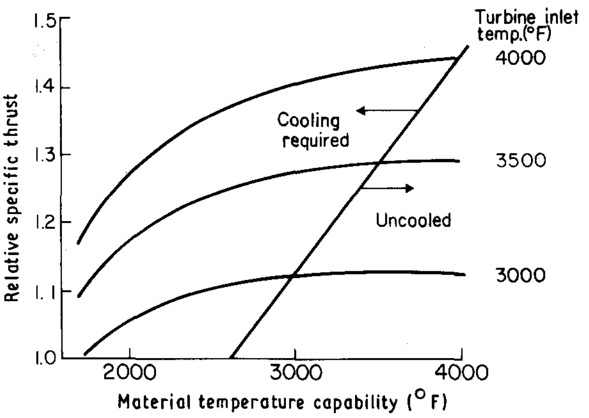

Figure 17 Effect of material operating temperature capability, turbine inlet temperature and cooling requirements on relative specific thrust of turbojet and turbofan engines (dry turbojet, OPR = 30 at SCS, constant cooling) [239]. °C = (°F − 32)/1.8.

With these sobering comments behind us, we can again look at Table II [34] and see the projections for titanium aluminide use in advanced gas-turbine engine concepts. The higher operating temperatures afforded by use of the titanium aluminides can be seen in terms of the enhancement in relative specific thrust in Fig. 17 [239], and from a cost viewpoint in that a 100 °F (56 °C) increase in operating temperature could result in a decrease of about $1m per military aircraft in life-cycle costs [318, 319]. In fact, it has been stated that "titanium [aluminide] based composites . . . are key to the achievement of the goals of the US Integrated High Performance Turbine Engine Technology (IHPTET) advanced engine program" [280], a sentiment echoed in other countries in developing advanced engines [281]. The titanium aluminides are also strong contenders for use on transatmospheric vehicles such as the US National Aerospace Plane (NASP) and on similar vehicles under consideration in other parts of the world [282, 283]. However, the first production application of the titanium aluminides could come in a terrestrial turbocharger [320].

7.1. Material maturity

In the perspective of the discussions regarding material maturity [316] and the mechanical properties presented in sections 3 (monolithic) and 5 (composites), the authors have summarized their perspective of the maturity of the titanium aluminides in Table VII. However, only with continued major research and development efforts to enhance behaviour, and emphasis on processing particularly to control cost, will even this time-table be achieved – but the pay-off, especially in demanding flying applications, is great when implementation occurs.

7.2. Fabrication

The primary (ingot production, casting, ingot breakdown, powder metallurgy) and secondary (forming,

TABLE VII Material maturation

Material class	Maturity[a]	Year of first application	
		Non-demanding[b]	Demanding[c]
α_2	7	1992	2000
α_2/MMC	4	1995[d]	2005
γ	2	1992	2010
γ/MMC	1	1995[d]	> 2010

[a] This involves chemistry and microstructure (and fibre/coating): 10: fully defined, 1: optimum parameters presently unknown.

[b] Terrestrial or non-life-dependent flying application.

[c] Critical life-dependent flying application.

[d] Demonstration use rather than utilizing novel characteristics of composite.

machining, chemical milling, etc.) fabrication of monolithic α_2 seem to be a (more difficult) extension of conventional titanium processing. A number of innovative processing techniques such as cold rolling of foil offer interesting opportunities [321, 322]. Monolithic γ is considerably more difficult to work than α_2 and may require NNS processes such as castings, powder metallurgy [180] or isothermal forging. There are indications, however, that control of chemistry and grain size can enhance hot workability and superplasticity (> 400% tensile elongation) [125, 323, 324].

Composite α_2 material can be fabricated by a number of techniques, although incompatibility problems (CTE differences and chemical reaction) remain with current fibre–matrix material concepts. Assuming these problems can be solved or circumvented, cost may dictate use. It has been suggested that the current cost of α_2 MMCs ($4000–5000 per lb or $8.8–11.0 per g) must be reduced to < $1000 per lb ($2.2 per g) for extensive application to occur [325]. Plasma spray approaches appear to offer the greatest potential for acceptable quality/cost product [180, 325]; however, when we add compliance/diffusion barrier coatings to current concepts it is clear that this cost goal is a major challenge.

7.3. Mechanical properties

The present discussion will follow the path taken by Larsen *et al.* [83] and only consider monolithic and

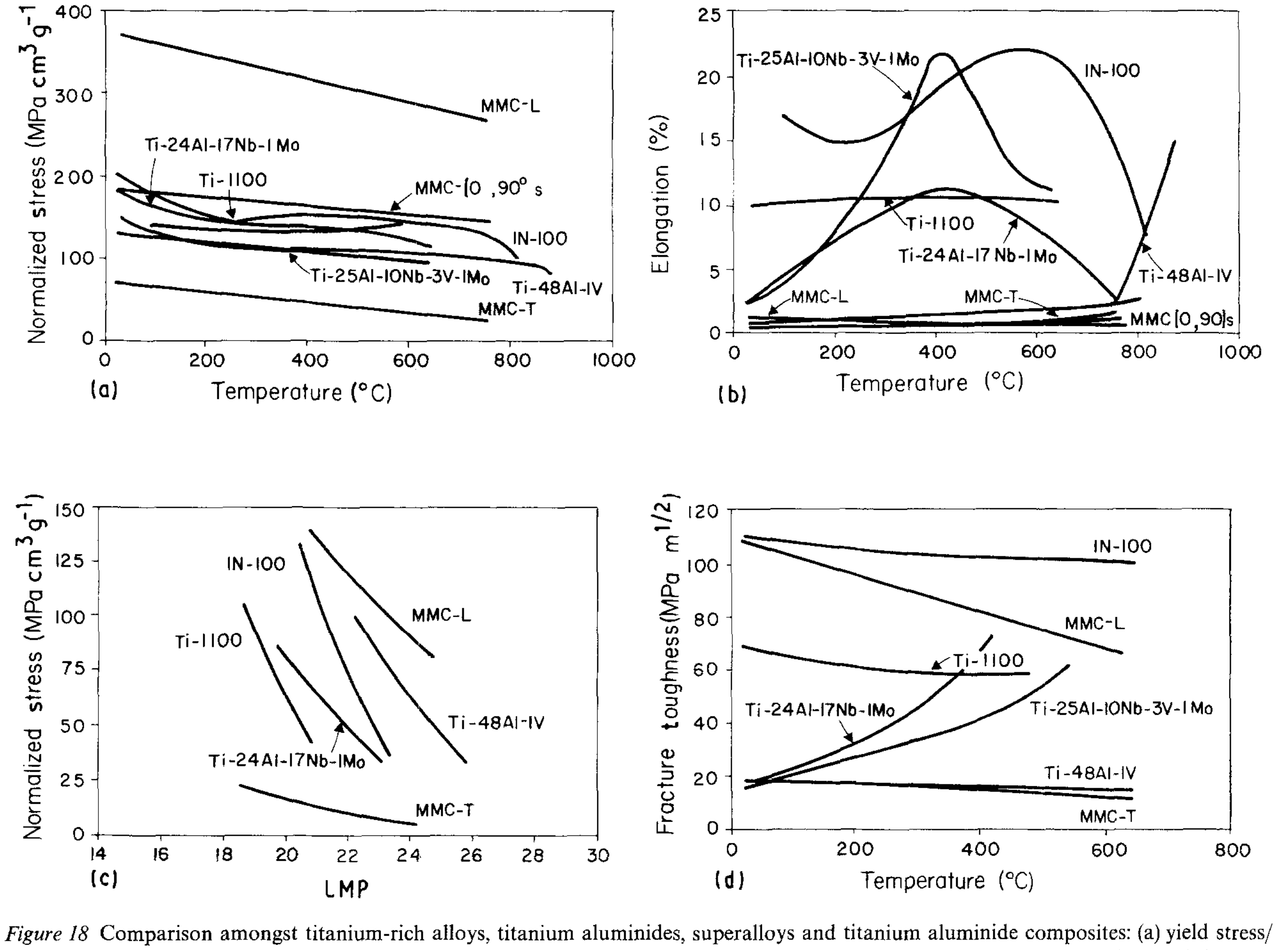

Figure 18 Comparison amongst titanium-rich alloys, titanium aluminides, superalloys and titanium aluminide composites: (a) yield stress/density versus temperature, (b) tensile elongation versus temperature, (c) Larson–Miller parameter normalized for rupture life and (d) fracture toughness versus temperature [83]. LMP = T (K) $\{20 + \log[t(\mathrm{h})]\}/1000$.

composite α_2 and solely monolithic γ, although for the future γ-composites may be viable. Comparisons of the monolithic and composite Ti_xAl material with conventional materials are shown in Fig. 18 [83].

The ductility of α_2-based alloys has been increased particularly with additions of Nb [82, 83]. However, Charpy impact toughness values are low, raising questions surrounding impact resistance (e.g. foreign object damage) [83]. Surface cracking can occur after long-time exposure to static or cyclic loading, reducing the overall ductility. However, fatigue life can be enhanced with the use of protective coatings [326]. The recently developed Ti–24Al–17Nb–1Mo composition [91] exhibits an enhanced combination of elevated-temperature strength and creep performance with room-temperature ductility and fracture toughness amongst the best obtained for α_2-type compositions. A further attraction of this composition is the increase in fracture toughness with temperature, from 19 MPa m$^{1/2}$ at RT to 50 MPa m$^{1/2}$ at 300 °C [83, 91]. Further, much is still to be done in optimizing the microstructure [112].

The α_2 composites demonstrate clear advantages over the monolithic alloy in the longitudinal direction, with excellent elevated-temperature strength and stiffness and a significant enhancement in fracture and fatigue crack growth resistance [83]. Russ [263] has convincingly demonstrated the "devastating" [83] effects of thermal fatigue in air, suggesting that in addition to the necessity for innovative design concepts, environmental effects will require resolution with the α_2 composites. Further, tailoring of the matrix for composite assemblies, rather than taking "off-the-shelf" monolithic alloys, should be pursued. Clearly the Ti–15Al–22.5Nb alloy shown in Table V [86, 91] with a fracture toughness of 42.3 MPa m$^{1/2}$ and an RT elongation of 6.7% is a good point at which to start, along with improved processing [112].

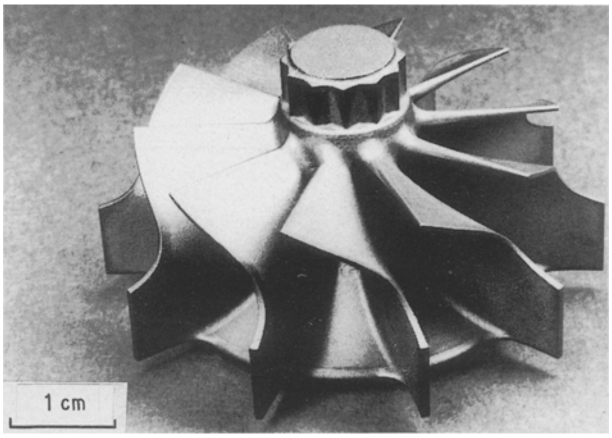

Figure 19 TiAl cast turbocharger rotor [320].

The monolithic γ alloys combine attractive elevated-temperature strength, creep performance and environmental resistance with high stiffness and low density. However, ductility at best slightly exceeds 2% at room temperature. It is also highly likely that impact resistance will be very low, probably precluding use in applications such as turbine blades [83]. Thus, it may well be that this class of materials is restricted to use in non-critical aerospace applications and terrestrial use such as automobile turbochargers.

7.4. Database

Neither the monolithic nor composite titanium aluminides have yet reached a state of maturity at which we can state that we have "optimum" material. Thus essentially nothing has yet been developed in terms of a database for these materials. Even with "innovations in the areas of structural design and life prediction . . .

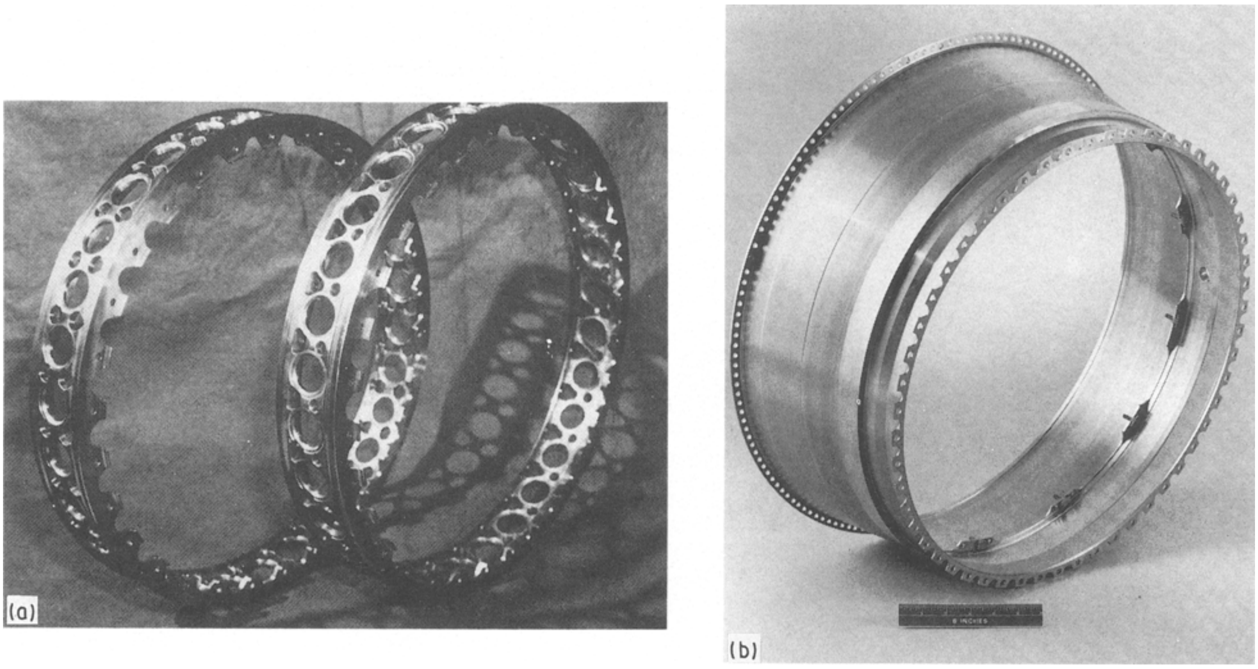

Figure 20 (a) High-pressure turbine stator inner support rings for a GE demonstrator engine, run for 25 h and (b) high-pressure compressor casing section, P & W F100 engine, run for 65 h [27].

to effectively utilize the unique properties of the titanium aluminides" [83] this class of materials must still comply with USAF structural integrity concepts [327]. This requires new materials to achieve certain predictable developmental milestones, including a substantial database, as they progress from the laboratory to use in full-scale production hardware.

7.5. Applications

To date there are no flying applications of the titanium aluminides. It does appear, however, that the γ composition will soon go into production in a turbocharger rotor [320]. The reduced weight of the cast TiAl rotor (Fig. 19) compared to a superalloy resulted in a more positive response, and the increased toughness compared to ceramics gave a much more durable product. Investigation of binary compositions revealed that a Ti–47Al alloy had the best combination of room-temperature and 900 °C properties (> 2% elongation at room temperature). Studies of tertiary additions were then followed by successful testing of a TiAl component. The authors indicate that commercialization of the TiAl rotor for automotive turbochargers is imminent.

A number of Ti_3Al and TiAl jet engine components have been produced successfully using casting and ingot approaches [27, 328] although, according to the open literature, none have yet flown; however, it is likely that non-critical parts will fly soon [124]. The parts shown in Fig. 20 are a high-pressure stator inner support ring, in which use of Ti_3Al saves 43% in weight compared to a superalloy part, and a high-pressure compressor casing section [27]. Other parts produced include PM and forged TiAl low-pressure turbine blades (Fig. 21 [124]). The direct HIP PM approach has been used to successfully produce impellers from Ti_3Al–Nb compositions (Fig. 8a) and rotors made from TiAl (Fig. 8b) [180].

The reinforced aluminides offer even greater potential for weight savings [280, 281]. This is the situation for components such as complex shaped blades, but even more so in ax-symmetrical parts such as rings, castings and discs where the filament direction can be oriented so that the large hoop stresses are accommodated by these filaments. The dramatic weight saving which can be achieved (up to 75%) by replacing

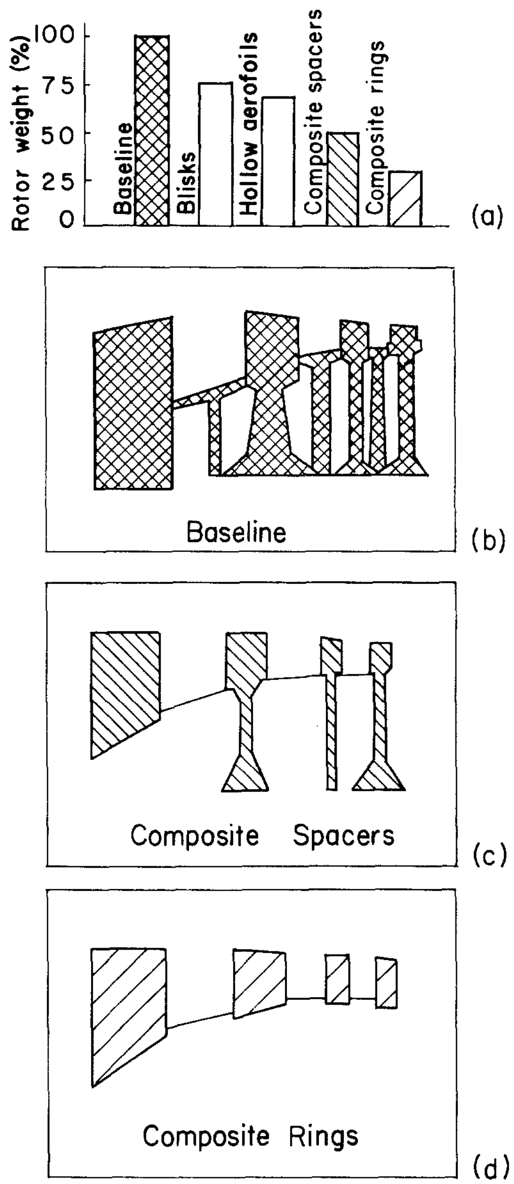

Figure 22 The weight savings which can be achieved (up to 75%) by replacing a conventional disc and spacer assembly with a titanium aluminide composite ring [281].

Figure 21 Turbine blade produced from TiAl using a powder metallurgy and hot forging approach [124].

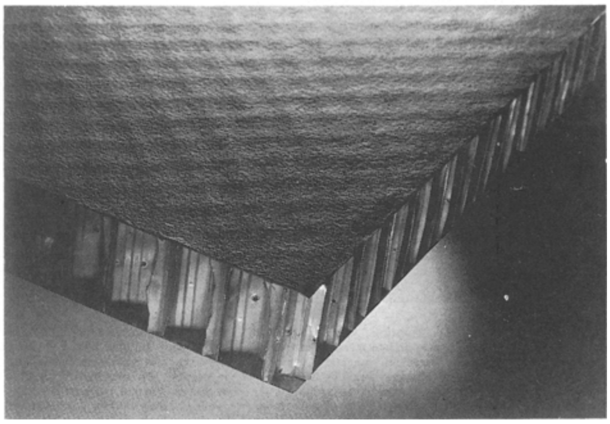

Figure 23 Honeycomb panel constructed of Ti–24Al–11Nb face sheets and Ti–3Al–$2\frac{1}{2}$V core [329].

a conventional disc and spacer assembly with a titanium aluminide reinforced ring is shown in Fig. 22 [281].

Both monolithic and composite titanium aluminides are being seriously considered for use on trans-atmospheric vehicles such as the NASP [282, 283]. Here applications could include skin surfaces, internal structural parts, rocket nozzles and engine parts [283]. An example of a honeycomb structure fabricated using an enhanced diffusion bonding process is shown in Fig. 23 [329].

8. Remaining challenges and conclusions

Because of their low density and attractive high-temperature behaviour the monolithic and composite titanium aluminides could replace superalloys in many elevated-temperature terrestrial, airframe, engine and missile applications. However, the great importance attached to structural integrity in advanced engine and airframe designs means that reliability and reproducibility are receiving increasing emphasis, and the low levels of "forgiveness" in the titanium aluminides is of major concern. At the present time there are no commercial applications of the titanium aluminides although many components have been fabricated from both the α_2 and γ alloys and have performed quite satisfactorily in ground-based tests. It is likely that we will see terrestrial and flying applications of the titanium aluminides in the near future, initially in non-critical components.

Much progress has been made but there are many remaining road-blocks and challenges to implementation. These include

(i) definition of an optimum α_2 monolithic composition/microstructure (combining acceptable ductility and creep and other mechanical properties);

(ii) full definition of interstitial effects on "forgiveness", particularly oxygen;

(iii) resolution of the toughness versus ductility requirement;

(iv) resolution of primary creep concerns;

(v) definition of an optimum γ monolithic composition/microstructure (combining acceptable ductility and creep and other mechanical properties);

(vi) evaluation of structures with elongated grains and single-crystal concepts;

(vii) development of a much better understanding of chemistry–processing–microstructure–mechanical property relationships for both α_2 and γ alloys, including nanostructure material (5% room temperature elongation in γ);

(viii) definition of an optimum α_2 MMC material with a more ductile, environmentally resistant matrix (using chemistry and microstructure as variables);

(ix) high quality, cost-effective, reproducible, compatible fibres/coatings (CTE and chemical reactivity) of the right diameter (generally thinner than the present $\sim 150\ \mu$m SCS-6 fibre) for various applications;

(x) more than one production fibre source;

(xi) development of (micromechanical) modelling capabilities for composites;

(xii) innovative design with these new "brittle" and anisotropic (MMC) materials;

(xiii) development of an adequate database on "optimum" material;

(xiv) resolution of environmental issues, especially for the composites;

(xv) a total engineering approach, incorporating life-cycle costs as well as acquisition costs;

(xvi) definition of secondary processing issues such as welding, joining, and forming;

(xvii) full-scale component manufacture and testing;

(xviii) demonstration flying applications, initially in non-critical parts; and

(xix) production of cost-affordable material.

Acknowledgements

In compiling this paper the authors acknowledge the help provided by T. Bales, S. Balsone, P. Bania, A. Begg, M. Blackburn, P. Blenkinsop, H. B. Bomberger, P. K. Brindley, J. C. Chesnutt, L. Christodoulou, R. Delagi, D. Driver, H. Gray, E. K. Hoffman, Y-W. Kim, J. M. Larsen, H. Lipsitt, R. A. Mackay, M. Mittnick, A. Molotkov, H. Nelson, J. Newman, A. B. Notkin, H. Oikawa, I. S. Polkin, T. M. F. Ronald, S. Russ, S. M. L. Sastry, J. Sorensen, N. I. Toby, R. Z. Valiev, S. Whang, J. C. Williams, C. F. Yolton and Dunxu Zou. Thanks are also given to Mrs Kandy Nelson, Mrs Susan L. Goetz, Mrs Leslie Cossairt and Mrs Virginia Foote for assistance in manuscript preparation.

References

1. Congress of the US, Office of Technology Assessment, "Advanced Materials by Design" (June 1988).
2. A. R. C. WESTWOOD, *Met. Trans. B.* **19B** (1988) 155.
3. F. H. FROES, in "P/M in Aerospace and Defense Technologies", edited by F. H. Froes (MPIF, Princeton, New Jersey, 1990) p. 23.
4. F. H. FROES, in Proceedings of ASM International sponsored meeting "Powder Metallurgy – Key to Advanced Materials Technology", Vancouver, July/August 1990, in press.
5. *Sci. Amer.* **255**(4) (1986).
6. F. H. FROES, in Proceedings of 4th Israel Materials Engineering Conference, edited by D. Itzhak and D. Eliezer (Weizmann Science Press of Israel, Jerusalem, 1989) pp. 1–41.
7. *Idem, Mater. Design* **10**(3) (1989) 110.
8. *Idem, Swiss Mater.* **2**(2) (1990) 23.
9. *Idem, Mater. Edge* **5** (1988) 19.
10. *Idem*, in "Advanced Materials – Outlook and Information Requirements", edited by L. J. Sousa and C. A. Sorrell (US BOM, Washington, DC, 1990) p. 41.
11. F. H. FROES, C. SURYANARAYANA and P. H. SHINGU, University of Idaho/Kyoto University, work in progress (1989–91).
12. F. H. FROES, *Mater. Edge* **6** (May/June 1989) 17.
13. F. H. FROES and C. SURYANARAYANA, in Proceedings of Workshop on Advanced Materials, Minsk, USSR, May/June 1989, in press.
14. F. H. FROES, in "Space Age Metals Technology", edited by F. H. Froes and R. A. Cull (SAMPE, Covina, California, 1988) p. 1.
15. F. H. FROES and Y. W. KIM, in Proceedings of International Conference on Advanced Materials, Milan, May 1989, in press.

16. C. SURYANARAYANA and F. H. FROES, *Light Metal Age* **47** (5/6) (1989) 18.
17. F. H. FROES and J. WADSWORTH, in Proceedings of BNF 7th International Conference, Oxford, UK, June 1989, in press.
18. R. W. CAHN, *Metals, Mater. Processes* **1** (1989) 1.
19. D. L. ANTON, D. M. SHAH, D. N. DUHL and A. F. GIAMEI, *JOM* **41**(9) (1989) 12.
20. R. L. FLEISCHER, D. M. DIMIDUK and H. A. LIPSITT, *Ann. Rev. Mater. Sci.* **19** (1989) 231.
21. R. L. FLEISCHER and A. I. TAUB, *JOM* **41**(9) (1989) 8.
22. N. S. STOLOFF and R. G. DAVIES, *Progr. Mater. Sci.* **13** (1966) 1.
23. J. H. WESTBROOK (ed.), "Mechanical Properties of Intermetallic Compounds" (Wiley, New York, 1960).
24. *Idem* (ed.), "Intermetallic Compounds" (Wiley, New York, 1967).
25. B. H. KEAR, C. T. SIMS, N. S. STOLOFF and J. H. WESTBROOK (eds), "Ordered Alloys – Structural Applications and Physical Metallurgy" (Claitor, Baton Rouge, Louisiana, 1970).
26. F. H. FROES, D. EYLON and H. B. BOMBERGER (eds), "Titanium Technology: Present Status and Future Trends" (Titanium Development Association, Dayton, Ohio, 1985).
27. H. A. LIPSITT, in "High Temperature Ordered Intermetallic Alloys", series Vol. 39, edited by C. C. Koch, C. T. Liu and N. S. Stoloff (MRS, Pittsburgh, 1985) p. 351.
28. M. J. BLACKBURN and M. P. SMITH, Technical Report AFWAL-TR-80-4175 (WPAFB, Ohio, 1980).
29. *Idem*, Technical Report AFWAL-TR-82-4086 (WPAFB, Ohio, 1982).
30. Y-W. KIM, *JOM* **41**(7) (1989) 24.
31. Y-W. KIM and F. H. FROES, in "High Temperature Aluminides and Intermetallics", edited by S. H. Whang, C. T. Liu, D. P. Pope and J. O. Stiegler (TMS, Warrendale, Pennsylvania, 1990) p. 485.
32. C. T. LIU, F. H. FROES and J. O. STIEGLER, in "Metals Handbook", 10th Edn, Vol. 2 (ASM International, Materials Park, Ohio, 1990) p. 913.
33. Y-W. KIM, in Proceedings "High Temperature Ordered Intermetallic Alloys IV", series Vol. 213, edited by L. A. Johnson, D. P. Pope and J. O. Stiegler (MRS, Pittsburgh, Pennsylvania, 1991) p. 777.
34. E. F. BRADLEY, in Proceedings of Gorham Advanced Materials Institute Conference, "Investment, Licensing and Strategic Partnering Opportunities, Emerging Technology, Applications, and Markets for Aluminides, Iron, Nickel and Titanium", Monterey, California, November 1989.
35. R. E. SCHAFRIK, *Met. Trans.* **8A** (1977) 1003.
36. N. S. CHOUDHURY, H. C. GRAHAM and J. W. HINZE, *J. Electrochem. Soc.* **123** (1976) 668.
37. M. KHOBAIB and F. W. VAHLDIEK, in "Space Age Metals Technology", edited by F. H. Froes and R. A. Cull (SAMPE, Covina, California, 1988) p. 262.
38. J. SUBRAHMANYAM, *J. Mater. Sci.* **23** (1988) 1906.
39. C. G. PANTANO and E. J. H. CHEN (eds), "Interfaces in Composites" (MRS, Pittsburgh, 1990).
40. R. B. BHAGAT, A. H. CLAUER, P. KUMAR and A. M. RITTER (eds), "Metal and Ceramic Matrix Composites: Processing, Modeling and Mechanical Behavior" (TMS, Warrendale, Pennsylvania, 1990).
41. D. L. ANTON, P. L. MARTIN, D. B. MIRACLE and R. McMEEKING (eds), "Intermetallic Matrix Composites", series Vol. 194 (MRS, Pittsburgh, 1990).
42. R. Y. LIN, R. J. ARSENAULT, G. P. MARTINS and S. G. FISHMAN (eds), "Interfaces in Metal–Ceramic Composites" (TMS, Warrendale, Pennsylvania, 1990).
43. C. C. KOCH, C. T. LIU and N. S. STOLOFF (eds), "High-Temperature Ordered Intermetallic Alloys", series Vol. 39 (MRS, Pittsburgh, 1985).
44. N. S. STOLOFF, C. C. KOCH, C. T. LIU and O. IZUMI (eds), "High-Temperature Ordered Intermetallic Alloys II", series Vol. 81 (MRS, Pittsburgh, 1987).
45. C. T. LIU, A. I. TAUB, N. S. STOLOFF and C. C. KOCH (eds), "High-Temperature Ordered Intermetallic Alloys III", series Vol. 133 (MRS, Pittsburgh, 1989).
46. S. H. WHANG, C. T. LIU, D. P. POPE and J. O. STIEGLER (eds), "High-Temperature Aluminides and Intermetallics" (TMS, Warrendale, Pennsylvania, 1990).
47. L. A. JOHNSON, D. P. POPE and J. O. STIEGLER (eds), "High-Temperature Ordered Intermetallic Alloys IV", series Vol. 213 (MRS, Pittsburgh, 1991).
48. J. B. McANDREW and D. McPHERSON, WADC-TR-53-182, Part II (WPAFB, Ohio, 1955) and *Trans. AIME* **206** (1956) 1348.
49. J. B. McANDREW and C. R. SIMCOE, WADD-TR-60-99 (WPAFB, Ohio, 1960).
50. E. Van ERKELENZ, *Metall. Erz.* **20**(11) (1923) 206.
51. W. MANCHOT and A. LEBER, *Z. Anorg. Chem.* **150** (1926) 26.
52. H. R. OGDEN, D. J. MAYKUTH, W. L. FINLAY and R. I. JAFFEE, *Trans. AIME* **191** (1951) 1150.
53. E. S. BUMPS, H. D. KESSLER and M. HANSEN, *ibid.* **194** (1952) 609.
54. I. I. KORNILOV, E. N. PYLAEVA and M. A. VOLKOVA, *Akad. Nauk SSSR, Otd. Khim. Nauk* **7** (1956) 771.
55. E. ENCE and H. MARGOLIN, *Trans. AIME* **221** (1961) 151.
56. I. I. KORNILOV, E. N. PYLAEVA, M. A. VOLKOVA, P. I. KRIPYAKEVICH and V. Y. MAEKIV, *Dokl. Akad. Nauk SSSR* **161** (1965) 843.
57. A. RAMAN and K. SCHUBERT, *Z. Metallkde* **56** (1965) 44.
58. M. J. BLACKBURN, *Trans. AIME* **239** (1967) 1200.
59. F. J. J. Van LOO and G. D. RIECK, *Acta Metall.* **21** (1973) 73.
60. R. D. SHULL, A. J. McALISTER and R. RENO, in "Titanium Science and Technology", Vol. 4, edited by G. Lutjering, U. Zwicker and W. Bunk (DGM, Oberursel, Germany, 1985) p. 1459.
61. J. L. MURRAY, "Phase Diagrams of Binary Titanium Alloys" (ASM International, Materials Park, Ohio, 1987) p. 12.
62. *Idem*, *Met. Trans.* **19A** (1988) 243.
63. C. McCULLOGH, J. J. VALENCIA, H. MATOES, C. G. LEVI, R. MEHRABIAN and K. A. RHYNE, *Scripta Metall.* **22** (1988) 1131.
64. C. McCULLOGH, J. J. VALENCIA, C. G. LEVI and R. MEHRABIAN, *Acta Metall.* **37** (1989) 1321.
65. S. C. HUANG and P. A. SIEMERS, *Met. Trans.* **20A** (1989) 1899.
66. R. G. ROWE and S. C. HUANG, *Israel J. Tech.* **24** (1988) 255.
67. S. C. HUANG, E. L. HALL and M. F. X. GIGLOTTI, in Proceedings of 6th World Conference on Titanium, Vol. 2, Cannes, France, June 1988, edited by P. Lacombe, R. Tricot and G. Beranger (Les Editions de Physique, Les Ulis Cedex, France, 1989) p. 1109.
68. K. KALTENBACH, S. GAMA, D. G. PINATTI, K. SCHULZE and E-T. HENIG, *Z. Metallkde.* **80** (1989) 535.
69. D. BANERJEE, T. K. NANDY, A. K. GOGIA and K. MURALEEDHARAN, in Proceedings of 6th World Conference on Titanium, Vol. 2, Cannes, France, June 1988, edited by P. Lacombe, R. Tricot and G. Beranger (Les Editions de Physique, Les Ulis Cedex, France, 1989) p. 1091.
70. M. J. KAUFMAN, T. F. BRODERICK, C. H. WARD, J. K. KIM, R. G. ROWE and F. H. FROES, in Proceedings of 6th World Conference on Titanium, Vol. 2, Cannes, France, June 1988, edited by P. Lacombe, R. Tricot and G. Beranger (Les Editions de Physique, Les Ulis Cedex, France, 1989) p. 985.
71. T. J. JEWETT, J. C. LIN, N. R. BONDA, L. E. SEITZMAN, K. C. HSIEH, Y. A. CHANG and J. H. PEREPEZKO, in "High-Temperature Ordered Intermetallic Alloys III", series Vol. 133, edited by C. T. Liu, A. I. Taub, N. S. Stoloff and C. C. Koch (MRS, Pittsburgh, 1989) p. 69.
72. T. TSUJIMOTO and K. HASHIMOTO, *ibid.* p. 391.
73. J. H. PEREPEZKO, Y. A. CHANG, L. E. SEITZMAN, J. C. LIN, N. R. BONDA, T. J. JEWETT and J. C. MISHURDA, in "High-Temperature Aluminides and Inter-

metallics", edited by S. H. Whang, C. T. Liu, D. P. Pope and J. O. Stiegler (TMS, Warrendale, Pennsylvania, 1990) p. 19.

74. C. SURYANARAYANA and D. S. LEE, *Scripta Metall.* in press.

75. R. STRYCHOR, J. C. WILLIAMS and W. A. SOFFA, *Met. Trans.* **19A** (1988) 225.

76. A. G. JACKSON, K. R. TEAL, D. EYLON, F. H. FROES and S. J. SAVAGE, in "Rapidly Solidified Alloys and Their Mechanical and Magnetic Properties", series Vol. 58, edited by B. C. Giessen, D. E. Polk and A. I. Taub (MRS, Pittsburgh, 1986) p. 365.

77. T. F. BRODERICK, K. R. TEAL and F. H. FROES, unpublished work, WPAFB, Ohio (1987).

78. D. BANERJEE, A. K. GOGIA, T. K. NANDI and V. A. JOSHI, *Acta Metall.* **36** (1988) 871.

79. L. A. BENDERSKY, W. J. BOETTINGER, B. P. BURTON, F. S. BIANCANIELLO and C. B. SHOEMAKER, *ibid.* **38** (1990) 931.

80. P. VILLARS and L. D. CALVERT, "Pearson's Handbook of Crystallographic Data for Intermetallic Phases" (ASM International, Metals Park, Ohio, 1985).

81. K. MURALEEDHARAN, S. V. NAGENDER NAIDU and D. BANERJEE, *Scripta Metall.* **24** (1990) 27.

82. R. G. ROWE, in "High-Temperature Aluminides and Intermetallics", edited by S. H. Whang, C. T. Liu, D. P. Pope and J. O. Stiegler (TMS, Warrendale, Pennsylvania, 1990) p. 375.

83. J. M. LARSEN, K. A. WILLIAMS, S. J. BALSONE and M. A. STUCKE, *ibid.* p. 521.

84. M. J. BLACKBURN, D. L. RUCKLE and C. E. BEVAN, Technical Report AFML-TR-78-18 (WPAFB, Ohio, 1978).

85. M. J. BLACKBURN and M. P. SMITH, Technical Report AFWAL-TR-81-4046 (WPAFB, Ohio, 1981).

86. *Idem*, Interim Technical Report FR-19139 (United Technologies, East Hartford, Connecticut, 1988).

87. H. B. BOMBERGER, Technical Report WRDC-TR-89-4036 (WPAFB, Ohio, 1989).

88. H. A. LIPSITT, D. SHECHTMAN and R. E. SCHAFRIK, *Met. Trans.* **11A** (1980) 1369.

89. S. A. COURT, J. P. A. LOFVANDER, M. H. LORETTO and H. L. FRASER, *Phil. Mag.* **59** (1989) 379.

90. P. L. MARTIN, H. A. LIPSITT, N. T. NUHFER and J. C. WILLIAMS, in "Titanium 80: Science and Technology", Vol. 2, edited by H. Kimura and O. Izumi (TMS, Warrendale, Pennsylvania, 1980) p. 1245.

91. M. J. BLACKBURN and M. P. SMITH, Technical Report WRDC-TR-89-4095 (WPAFB, Ohio, 1989).

92. M. J. BLACKBURN and M. P. SMITH, US Patent 4 294 615 (1981).

93. M. J. BLACKBURN, J. T. HILL and M. P. SMITH, AFWAL-TR-84-4078 (WPAFB, Ohio, 1984).

94. P. K. BRINDLEY, S. L. DRAPER, M. V. NATHAL and J. I. ELDRIDGE, in "Fundamental Relationships Between Microstructure and Mechanical Properties of Metal Matrix Composites", edited by P. K. Liaw and M. N. Gungar (TMS, Warrendale, Pennsylvania, 1990) p. 387.

95. D. A. KOSS, D. BANERJEE, D. A. LUKASAK and A. K. GOGIA, in "High-Temperature Aluminides and Intermetallics", edited by S. H. Whang, C. T. Liu, D. P. Pope and J. O. Stiegler (TMS, Warrendale, Pennsylvania, 1990) p. 175.

96. J. W. NEWKIRK and G. B. FELDEWERTH, in "High-Temperature Ordered Intermetallic Alloys III", series Vol. 133, edited by C. T. Liu, A. I. Taub, N. S. Stoloff and C. C. Koch (MRS, Pittsburgh, 1989) p. 681.

97. C. H. WARD, J. C. WILLIAMS, A. W. THOMPSON, D. G. ROSENTHAL and F. H. FROES, in Proceedings of 6th World Conference on Titanium, Vol. 2, Cannes, France, June 1988, edited by P. Lacombe, R. Tricot and G. Beranger (Les Editions de Physique, Les Ulis Cedex, France, 1989) p. 1103.

98. A. K. GOGIA, T. K. NANDY, D. BANERJEE and Y. MAHAJAN, *ibid.* p. 1097.

99. J. C. WILLIAMS and M. J. BLACKBURN, in "Ordered Alloys", edited by B. H. Kear, C. T. Sims, N. S. Stoloff and J. H. Westbrook (Claitor, Baton Rouge, Louisiana, 1970) p. 425.

100. S. M. L. SASTRY and H. A. LIPSITT, *Met. Trans.* **8A** (1977) 1543.

101. *Idem*, in "Titanium 80: Science and Technology", Vol. 2, edited by H. Kimura and O. Izumi (TMS, Warrendale, Pennsylvania, 1980) p. 1231.

102. S. A. COURT, J. P. A. LOFVANDER, M. H. LORETTO and H. L. FRASER, *Phil. Mag.* **61** (1990) 109.

103. A. K. GOGIA, D. BANERJEE and T. K. NANDY, *Met. Trans.* **21A** (1990) 609.

104. M. THOMAS, A. VASSEL and P. VEYSSIERE, *Scripta Metall.* **21** (1987) 501.

105. B. J. MARQUARDT, G. K. SCARR, J. C. CHESTNUT, C. G. RHODES and H. L. FRASER, in Proceedings of 6th World Conference on Titanium, Vol. 2, Cannes, France, June 1988, edited by P. Lacombe, R. Tricot and G. Beranger (Les Editions de Physique, Les Ulis Cedex, France, 1989) p. 955.

106. J. P. A. LOFVANDER, S. A. COURT, M. H. LORETTO and H. L. FRASER, *Phil. Mag. Lett.* **60**, (1989) 111.

107. J. C. WILLIAMS, in "Titanium and Titanium Alloys", Vol. 2, edited by J. C. Williams and A. F. Belov (Plenum, New York, 1982) p. 1477.

108. J. C. WILLIAMS, B. S. HICKMAN and H. L. MARCUS, *Met. Trans.* **2** (1971) 1913.

109. D. BANERJEE, A. K. GOGIA and T. K. NANDY, *ibid.* **21A** (1990) 627.

110. K. CHO and J. GURLAND, *ibid.* **19A** (1988) 2027.

111. A. K. GOGIA, T. K. NANDY, D. BANERJEE and Y. MAHAJAN, in Proceedings of 6th World Conference on Titanium, Vol. 2, Cannes, France, June 1988, edited by P. Lacombe, R. Tricot and G. Beranger (Les Editions de Physique, Les Ulis Cedex, France, 1989) p. 1097.

112. ZOU DUNXU, Central Iron and Steel Research Institute, Beijing, Private Communication (1991).

113. D. A. LUKASAK and D. A. KOSS, *Met. Trans.* **21A** (1990) 135.

114. R. W. HERTZBERG, "Deformation and Fracture Mechanics of Engineering Materials, 2nd Ed (Wiley, New York, 1983).

115. M. A. STUCKE and H. A. LIPSITT, in "Titanium Rapid Solidification Technology", edited by F. H. Froes and D. Eylon (TMS, Warrendale, Pennsylvania, 1986) p. 255.

116. W. CHO, "Effect of Microstructure on Deformation and Creep Behavior of Ti–25Al–10Nb–3V–1Mo", Technical Report (Air Force Office of Scientific Research, Bolling Air Force Base, Washington, DC, 1988).

117. C. G. RHODES, in Proceedings of 6th World Conference on Titanium, Vol. 1, Cannes, France, June 1988, edited by P. Lacombe, R. Tricot and G. Beranger (Les Editions de Physique, Les Ulis Cedex, France, 1989) p. 199.

118. M. G. MENDIRATTA and H. A. LIPSITT, *J. Mater. Sci.* **15** (1980) 2985.

119. S-C. HUANG and E. L. HALL, in "High-Temperature Ordered Intermetallic Alloys III", series Vol. 133, edited by C. T. Liu, A. I. Taub, N. S. Stoloff and C. C. Koch (MRS, Pittsburgh, 1989) p. 373.

120. T. TSUJIMOTO and K. HASHIMOTO, *ibid.* p. 391.

121. C. R. FENG, D. J. MICHEL and C. R. CROWE, *ibid.* p. 669.

122. I. A. ZELONKOV and Ye. N. MARTYNCHIK, *Metallofizika, Naukova Dumka* **42** (1972) 63.

123. T. KAWABATA, M. TADANO and O. IZUMI, *Scripta Metall.* **22** (1988) 1725.

124. A. B. NOTKIN and A. MOLOTKOV, All Union Institute for Light Alloys, Moscow, Private Communication (1991).

125. R. Z. VALIEV, Institute for Metals Superplasticity Problems, USSR Academy of Sciences, Khalturina, Private Communication (1991).

126. T. KAWABATA, T. KANAI and O. IZUMI, *Acta Metall.* **33** (1985) 1355.

127. S. H. WHANG and Y. D. HAHN, *Scripta Met. Mater.* **24** (1990) 485.

128. D. SHECHTMAN, M. J. BLACKBURN and H. A. LIPSITT, *Met. Trans.* **5** (1974) 1373.

129. H. A. LIPSITT, D. SHECHTMAN and R. E. SCHAFRIK, *ibid.* **6A** (1975) 1991.

130. T. KAWABATA and O. IZUMI, in "High-Temperature Aluminides and Intermetallics", edited by S. H. Whang,

C. T. Liu, D. P. Pope and J. O. Stiegler (TMS, Warrendale, Pennsylvania, 1990) p. 403.

131. S. H. WHANG and Y. D. HAHN, *ibid.* p. 91.
132. B. A. GREENBERG, O. V. ANTONOVA, V. N. INDENBAUM, L. E. KARKINA, A. B. NOTKIN and M. V. PONOMAREV, Preprint No. 89/7 (USSR Academy of Sciences Ural Division, Sverdlovsk, 1989).
133. M. J. MARCINKOWSKI, N. BROWN and R. M. FISCHER, *Acta Metall.* **9** (1961) 129.
134. G. HUG, A. LOISEAU and P. VEYSSIERE, *Phil Mag.* **A57** (1988) 499.
135. S. H. WHANG and Y. D. HAHN, in "High-Temperature Ordered Intermetallic Alloys III", series Vol. 133, edited by C. T. Liu, A. I. Taub, N. S. Stoloff and C. C. Koch (MRS, Pittsburgh, 1989) p. 687.
136. S. C. HUANG and E. L. HALL, *ibid.* p. 373.
137. J. Y. KIM, Y. D. HAHN and S. H. WHANG, *Scripta Met. Mater.* **25** (1991) 548.
138. Y. D. HAHN and S. H. WHANG, *ibid.* **24** (1990) 139.
139. S. H. WHANG and Y. D. HAHN, *ibid.* **24** (1990) 1679.
140. Y. D. HAHN and S. H. WHANG, *Met. Trans. A* in press.
141. T. KAWABATA and O. IZUMI, *Scripta Metall.* **21** (1987) 435.
142. E. L. HALL and S. C. HUANG, in "High-Temperature Ordered Intermetallic Alloys III", series Vol. 133, edited by C. T. Liu, A. I. Taub, N. S. Stoloff and C. C. Koch (MRS, Pittsburgh, 1989) p. 693.
143. T. KAWABATA, M. TADANO and O. IZUMI, *Scripta Metall.* **22** (1988) 1725.
144. V. K. VASUDEVAN, S. A. COURT, P. KURATH and H. L. FRASER, *ibid.* **23** (1989) 907.
145. S. A. COURT, V. K. VASUDEVAN and H. L. FRASER, *Phil. Mag.* **A61** (1990) 141.
146. B. A. GREENBERG, *Phys. Status Solidi* (*b*) **55** (1973) 59.
147. T. FUJIWARA, A. NAKAMURA, M. HOSOMI, S. R. NISHITANI, Y. SHIRAI and M. YAMAGUCHI, *Phil. Mag.* **A61** (1990) 591.
148. T. HANAMURA and M. TANINO, *J. Mater. Sci. Lett.* **8** (1989) 24.
149. M. YAMAGUCHI, S. R. NISHITANI and Y. SHIRAI, in "High-Temperature Aluminides and Intermetallics", edited by S. H. Whang, C. T. Liu, D. P. Pope and J. O. Stiegler (TMS, Warrendale, Pennsylvania, 1990) p. 63.
150. R. A. AMATO, J. C. CHESNUTT, M. F. X. GIGLIOTTI, S. C. HUANG, D. G. KONITZER, M. M. LEE, R. G. ROWE, G. K. SCARR and P. A. ZOMCIK, Interim Report No. 6, Contract F33615-86-C-5073 (WPAFB, Ohio, 1989).
151. H. R. OGDEN, D. J. MAYKUTH, W. L. FINLAY and R. I. JAFFEE, *JOM* (February 1953) 267.
152. M. J. BLACKBURN and M. P. SMITH, AFML-TR-79-4056 (WPAFB, Ohio, 1979).
153. T. TSUJIMOTO, K. HASHIMOTO, M. NOBUKI and H. SUGA, *Trans. Jpn Inst. Metals* **27** (1986) 341.
154. S. M. BARINOV, T. T. NARTOVA, Y. L. KRASULIN and T. V. MOGUTOVA, *Izvestiya Akademii Nauk USSR* **5** (1983) 170.
155. T. TAKAHASHI and H. OIKAWA, in "High-Temperature Ordered Intermetallic Alloys III", series Vol. 133, edited by C. T. Liu, A. I. Taub, N. S. Stoloff and C. C. Koch (MRS, Pittsburgh, 1989) p. 699.
156. H. OIKAWA, in "High-Temperature Aluminides and Intermetallics", edited by S. H. Whang, C. T. Liu, D. P. Pope and J. O. Stiegler (TMS, Warrendale, Pennsylvania, 1990) p. 353.
157. H. B. BOMBERGER and F. H. FROES, in "Titanium Technology: Present Status and Future Trends", edited by F. H. Froes, D. Eylon and H. B. Bomberger (Titanium Development Association, Dayton, Ohio, 1985) p. 25.
158. T.E. O'CONNEL, AFWAL-TR-83-4050 (WPAFB, Ohio, 1983).
159. P. J. BANIA, Timet, Henderson, Nevada, Private Communications (1991).
160. H. B. BOMBERGER, US Patent 3 679 403 (1972).
161. *Idem*, US Patent 3 963 525 (1976).
162. *Idem*, US Patent 4 129 438 (1978).
163. R. M. GERMAN, "Powder Metallurgy Science" (MPIF, Princeton, 1984).
164. H. JONES, "Rapid Solidification of Metals and Alloys", Monograph No. 8 (Institution of Metallurgists, London, UK, 1982).
165. F. H. FROES and D. EYLON, *Int. Mater. Rev.* **35** (1990) 162.
166. F. H. FROES and R. G. ROWE, in "Rapidly Solidified Alloys and Their Mechanical and Magnetic Properties", series Vol. 58, edited by B. C. Giessen, D. E. Polk and A. I. Taub (MRS, Pittsburgh, 1986) p. 309.
167. T. R. ANANTHARAMAN and C. SURYANARAYANA, "Rapidly Solidified Metals – A Technological Overview" (Trans Tech, Aedermannsdorf, Switzerland, 1987).
168. F. H. FROES and R. G. ROWE, in Proceedings of 6th World Conference on Titanium, Vol. 2, Cannes, France, June 1988, edited by P. Lacombe, R. Tricot and G. Beranger (Les Editions de Physique, Les Ulis Cedex, France, 1989) p. 801.
169. C. SURYANARAYANA, F. H. FROES and R. G. ROWE, *Int. Mater. Rev.* **36** (1991) 85.
170. R. SUNDARESAN and F. H. FROES, *JOM* **39**(8) (1987) 22.
171. *Idem, Met. Powd. Rep.* **44** (1989) 195.
172. C. SURYANARAYANA, R. SUNDARESAN and F. H. FROES, in "Structural Applications of Mechanical Alloying", edited by F. H. Froes and J. J. deBarbadillo (ASM International, Materials Park, Ohio, 1990) p. 193.
173. R. R. ODDONE and R. M. GERMAN, in "Advances in Powder Metallurgy", edited by T. G. Gasbarre and W. F. Jandeska Jr (MPIF, Princeton, 1989) p. 475.
174. R. E. SCHAFRIK, *Met. Trans.* **7B** (1976) 713.
175. Ch. HARTIG, S. CHEN, P. A. BEAVEN and H. FUKUTOMI, in Proceedings of 6th World Conference on Titanium, Vol. 2, Cannes, France, June 1988, edited by P. Lacombe, R. Tricot and G. Beranger (Les Editions de Physique, Les Ulis Cedex, France, 1989) p. 1021.
176. D. D. BHATT, G. E. MEYER and A. L. HOFFMANNER, AFML-TR-87-59 (WPAFB, Ohio, 1978).
177. T. E. O'CONNELL and J. A. MILLER, Interim Technical Report AFML-TR-78-129 (WPAFB, Ohio, 1978).
178. P. R. ROBERTS, in "Advances in Powder Metallurgy", edited by T. G. Gasbarre and W. F. Jandeska Jr (MPIF, Princeton, 1989) p. 427.
179. A. P. WOODFIELD, R. A. AMATO and C. F. YOLTON, *ibid.* p. 413.
180. J. H. MOLL, C. F. YOLTON and B. J. McTIERNAN, *Int. J. Powd. Metall.* **26** (1990) 149.
181. F. H. FROES and R. G. ROWE, Unpublished Work, WPAFB, Ohio (1985–87).
182. C. SURYANARAYANA and F. H. FROES, University of Idaho, Moscow, Idaho, Work in Progress (1991).
183. F. H. FROES and D. EYLON (eds), "Titanium – Rapid Solidification Technology" (TMS, Warrendale, Pennsylvania, 1986).
184. F. H. FROES and S. J. SAVAGE, (eds), "Processing of Structural Metals by Rapid Solidification" (ASM International, Materials Park, Ohio, 1987).
185. F. H. FROES and R. G. ROWE, in "Titanium – Rapid Solidification Technology", edited by F. H. Froes and D. Eylon (TMS, Warrendale, Pennsylvania, 1986) p. 1.
186. H. B. BOMBERGER and F. H. FROES, *ibid.* p. 21.
187. R. G. ROWE and F. H. FROES, in "Processing of Structural Metals by Rapid Solidification", edited by F. H. Froes and S. J. Savage (ASM International, Materials Park, Ohio, 1987) p. 163.
188. C. SURYANARAYANA and F. H. FROES, *JOM* **42**(3) (1990) 22.
189. R. G. ROWE, J. A. SUTLIFF and E. F. KOCK, in "Titanium – Rapid Solidification Technology", edited by F. H. Froes and D. Eylon (TMS, Warrendale, Pennsylvania, 1986) p. 239.
190. R. G. ROWE, A. I. TAUB and F. H. FROES, in "Rapid Solidification Processing: Principles and Technologies IV", edited by R. Mehrabian and P. A. Parrish (Claitor, Baton Rouge, Louisiana, 1988) p. 149.
191. K. R. TEAL, A. G. JACKSON, D. EYLON and F. H. FROES, in "Titanium – Rapid Solidification Technology", edited by F. H. Froes and D. Eylon (TMS, Warrendale, Pennsylvania, 1986) p. 231.

192. R. G. ROWE, in Proceedings of 6th World Conference on Titanium, Vol. 2, Cannes, France, June 1988, edited by P. Lacombe, R. Tricot and G. Beranger (Les Editions de Physique, Les Ulis Cedex, France, 1989) p. 979.
193. C. H. WARD, T. F. BRODERICK, A. G. JACKSON, R. G. ROWE and F. H. FROES, in "Processing of Structural Metals by Rapid Solidification", edited by F. H. Froes and S. J. Savage (ASM International, Materials Park, Ohio, 1987) p. 243.
194. J. W. SEARS, J. P. A. LOFVANDER, R. WHEELER, M. A. STUCKE, S. A. COURT and H. L. FRASER, in Proceedings of 6th World Conference on Titanium, Vol. 2, Cannes, France, June 1988, edited by P. Lacombe, R. Tricot and G. Beranger (Les Editions de Physique, Les Ulis Cedex, France, 1989) p. 1115.
195. S. C. JHA, R. RAY, K. R. TEAL and F. H. FROES, *ibid.* p. 961.
196. J. A. SUTLIFF and R. G. ROWE, in "Rapidly Solidified Alloys and Their Mechanical and Magnetic Properties", series Vol. 58, edited by B. C. Giessen, D. E. Polk and A. I. Taub (MRS, Pittsburgh, 1986) p. 371.
197. G. VENKATARAMAN, A. G. JACKSON, K. R. TEAL and F. H. FROES, *Mater. Sci. Engng* **98** (1988) 257.
198. G. VENKATARAMAN, K. R. TEAL and F. H. FROES, in Proceedings of 6th World Conference on Titanium, Vol. 2, Cannes, France, June 1988, edited by P. Lacombe, R. Tricot and G. Beranger (Les Editions de Physique, Les Ulis Cedex, France, 1989) p. 967.
199. G. VENKATARAMAN, A. G. JACKSON and F. H. FROES, *ibid.* 973.
200. F. H. FROES and J. R. PICKENS, *JOM* **36**(1) (1984) 14.
201. F. H. FROES, Y-W. KIM and F. HEHMANN, *ibid.* **39**(8) (1987) 14.
202. C. SURYANARAYANA, F. H. FROES, S. KRISHNAMURTHY and Y-W. KIM, *Int. J. Powd. Metall.* **26** (1990) 117.
203. T. C. PENG, B. LONDON and S. M. L. SASTRY, in "Advances in Powder Metallurgy", edited by T. G. Gasbarre and W. F. Jandeska Jr (MPIF, Princeton, 1989) p. 387.
204. D. VUJIC, Z. X. LI and S. H. WHANG, *Met. Trans.* **19A** (1988) 2445.
205. S. C. HUANG, E. L. HALL and M. F. X. GIGLIOTTI, in "High-Temperature Ordered Intermetallic Alloys II", series Vol. 81, edited by N. S. Stoloff, C. C. Koch, C. T. Liu and O. Izumi (MRS, Pittsburgh, 1987) p. 481.
206. J. A. GRAVES, L. A. BENDERSKY, F. S. BIANCANIELLO, J. H. PEREPEZKO and W. J. BOETTINGER, *Mater. Sci. Engng* **98** (1988) 265.
207. C. McCULLOUGH, J. J. VALENCIA, C. G. LEVI and R. MEHRABIAN, *Scripta Metall.* **21** (1987) 1341.
208. J. A. GRAVES, J. H. PEREPEZKO, C. H. WARD and F. H. FROES, *ibid.* **21** (1987) 567.
209. J. C. MISHURDA, J. H. PEREPEZKO, J. A. GRAVES and F. H. FROES, in Proceedings of 6th World Conference on Titanium, Vol. 2, Cannes, France, June 1988, edited by P. Lacombe, R. Tricot and G. Beranger (Les Editions de Physique, Les Ulis Cedex, France, 1989) p. 1127.
210. D. S. SHIH, G. K. SCARR and J. C. CHESNUTT, in "High-Temperature Ordered Intermetallics III", series Vol. 133, edited by C. T. Liu, A. I. Taub, N. S. Stoloff and C. C. Koch (MRS, Pittsburgh, 1989) p. 167.
211. E. L. HALL and S. C. HUANG, GE Corporate R & D Center, Schenectady, NY, Work in Progress (1990–91).
212. S. C. HUANG, GE Corporate R & D Center, Schenectady, NY, Private Communication (1989).
213. E. L. HALL and S. C. HUANG, in "High-Temperature Ordered Intermetallic Alloys III", series Vol. 133, edited by C. T. Liu, A. I. Taub, N. S. Stoloff and C. C. Koch (MRS, Pittsburgh, 1989) p. 693.
214. C. SURYANARAYANA, R. SUNDARESAN and F. H FROES, in "Solid State Powder Processing", edited by A. H. Clauer and J. J. deBarbadillo (TMS, Warrendale, Pennsylvania, 1990) p. 55.
215. F. H. FROES and D. EYLON, in "Hydrogen Effects on Materials Behavior", edited by N. R. Moody and A. W. Thompson (TMS, Warrendale, Pennsylvania, 1990) p. 261.
216. F. H. FROES, D. EYLON and C. SURYANARAYANA, *JOM* **42**(3) (1990) 26.
217. L. S. STEELE, D. EYLON, K. R. TEAL, I. WEISS and F. H. FROES, in Proceedings of 6th World Conference on Titanium, Vol. 2, Cannes, France, June 1988, edited by P. Lacombe, R. Tricot and G. Beranger (Les Editions de Physique, Les Ulis Cedex, France, 1989) p. 1009.
218. L. S. STEELE, D. EYLON and F. H. FROES, in "Advances in Powder Metallurgy", edited by T. G. Gasbarre and W. F. Jandeska Jr (MPIF, Princeton, 1989) p. 509.
219. I. S. POLKIN, All Union Institute for Light Alloys, Moscow, USSR, Private Communication (1989).
220. D. S. SHONG, Y-W. KIM, C. F. YOLTON and F. H. FROES, in "High-Temperature Ordered Intermetallic Alloys III", series Vol. 133, edited by C. T. Liu, A. I. Taub, N. S. Stoloff and C. C. Koch (MRS, Pittsburgh, 1989) p. 711.
221. L. S. SIGL, P. A. MATAGA, J. DALGLEISH, R. M. McMEEKING and A. G. EVANS, *Acta Metall.* **36** (1988) 945.
222. M. S. NEWKIRK, A. W. URGHART and H. R. ZWICKER, *J. Mater. Res.* **1** (1986) 81.
223. I. AKSAY and A. PYSIK, in "Ceramic Microstructures: Role of Interfaces", edited by J. A. Pask and A. G. Evans (Plenum, New York, 1987) pp. 1–17.
224. J. BREME and Th. WEIK, in Proceedings of 6th World Conference on Titanium, Vol. 2, edited by P. Lacombe, R. Tricot and G. Beranger (Editions de Physique, Les Ulis Cedex, France, 1989) p. 1003.
225. C. K. ELLIOTT, G. R. ODETTE, G. E. LUCAS and J. W. SCHECKHERD, in "High Temperature/High Performance Composites", series Vol. 120, edited by F. D. Lemkey, A. G. Evans, S. G. Fishman and J. R. Strife (MRS, Pittsburgh, 1988) p. 95.
226. G. R. ODETTE, H. E. DÈVE, C. K. ELLIOTT, A. HASEGAWA and G. E. LUCAS, in "Interfaces in Metal–Ceramic Composites", edited by R. Y. Lin, R. J. Arsenault, G. P. Martins and S. G. Fishman (TMS, Warrendale, Pennsylvania, 1990) p. 443.
227. S. M. L. SASTRY and R. J. LEDERICH, McDonnell-Douglas Research Laboratories, St. Louis, reported at Conference on Current Topics on Intermetallics for Structural Applications, Neuchatel, Switzerland, March 1989.
228. J. C. LIN, Y. A. CHANG and J. H. PEREPEZKO, *Scripta Metall.* in press.
229. K. K. CHAWLA, "Composite Materials – Science and Technology" (Springer, New York, 1987).
230. D. M. DIMIDUK and D. B. MIRACLE, in "High-Temperature Ordered Intermetallic Alloys III", series Vol. 133, edited by C. T. Liu, A. I. Taub, N. S. Stoloff and C. C. Koch (MRS, Pittsburgh, 1989) p. 349.
231. P. R. SMITH and F. H. FROES, *JOM* **36**(3) (1984) 19.
232. *Idem, Chinese J. Mater. Engng* No. 3 (Sum No. 100) (June 1990) 1.
233. P. R. SMITH, F. H. FROES and J. CAMMETT, in "Mechanical Behavior of Metal Matrix Composites", edited by J. E. Hack and M. F. Amateau (TMS, Warrendale, Pennsylvania , 1983) p. 143.
234. *Aviation Week* (November 28 1988) 46.
235. M. MITTNICK, *SAMPE J.* **26**(5) (1990) 49.
236. M. A. MITTNICK and J. McELMAN, in Proceedings of 13th Conference on Metal Matrix Composites, Vol. 2, edited by J. D. Buckley, NASA Conference Publication No. 3054 (NASA, Washington, DC, 1990) p. 389.
237. M. MITTNICK and F. H. FROES, in "Metal Matrix Composites", edited by A. R. Begg (Arnold, Sevenoaks, Kent, UK, 1991).
238. P. K. BRINDLEY, in "High-Temperature Ordered Intermetallic Alloys II", series Vol. 81, edited by N. S. Stoloff, C. C. Koch, C. T. Liu and O. Izumi (MRS, Pittsburgh, 1987) p. 419.
239. D. L. McDANIELS and J. R. STEPHENS, NASA Technical Memorandum 100844 (Lewis Research Center, Cleveland, Ohio, 1988).
240. S. G. FISHMAN, in "Interfaces in Metal–Ceramic Composites", edited by R. Y. Lin, R. J. Arsenault, G. P. Martins

and S. G. Fishman (TMS, Warrendale, Pennsylvania, 1990) p. 3.

241. S. KRISHNAMURTHY, *ibid.* p. 75.
242. R. P. NIMMER, R. J. BARKERT, E. S. RUSSELL and G. A. SMITH, in Proceedings of ASM International Materials Week, October 1989, in press.
243. P. K. WRIGHT, R. NIMMER, G. SMITH, M. SONSMEIER and M. BRUN, in "Interfaces in Metal–Ceramic Composites", edited by R. Y. Lin, R. J. Arsenault, G. P. Martins and S. G. Fishman (TMS, Warrendale, Pennsylvania, 1990) p. 559.
244. D. S. SHONG, Y-W. KIM, C. F. YOLTON and F. H. FROES, in"Advances in Powder Metallurgy", edited by T. G. Gasbarre and W. F. Jandeska Jr (MPIF, Princeton, 1989) p. 359.
245. A. G. METCALFE and M. J. KLEIN, in "Composite Materials", Vol. 1, edited by A. G. Metcalfe (Academic, New York, 1974) p. 125.
246. A. G. METCALFE, *J. Compos. Mater.* **1** (1967) 356.
247. P. R. SMITH, C. G. RHODES and W. C. REVELOS, in "Interfaces in Metal–Ceramic Composites", edited by R. Y. Lin, R. J. Arsenault, G. P. Martins and S. G. Fishman (TMS, Warrendale, Pennsylvania, 1990) p. 35.
248. D. R. SCHUYLER, M. M. SOHI and R. MAHAPATRA, *ibid.* p. 475.
249. G. DAS and F. H. FROES, in Proceedings of 6th World Conference on Titanium, Vol. 2, Cannes, France, June 1988, edited by P. Lacombe, R. Tricot and G. Beranger (Les Editions de Physique, Les Ulis Cedex, France, 1989) p. 907.
250. G. DAS, in "Advances in Powder Metallurgy", edited by T. G. Gasbarre and W. F. Jandeska Jr (MPIF, Princeton, 1989) p. 491.
251. C. G. RHODES, M. S. VASSILIOU, M. R. MITCHELL and R. A. SPURLING, *Met. Trans.* **21A** (1990) 1589.
252. S. F. BAUMANN, P. K. BRINDLEY and S. D. SMITH, *ibid.* **21A** (1990) 1559.
253. D. E. BOSS and J. M. YANG, in "Intermetallic Matrix Composites", series Vol. 194, edited by D. L. Anton, P. L. Martin, D. B. Miracle and R. McMeeking (MRS, Pittsburgh, 1990) p. 429.
254. J. H. NORMAN, G. H. REYNOLDS and L. BREWER, *ibid.* p. 369.
255. S. M. JENG, C. J. YANG, J.-M. YANG, D. G. ROSENTHAL and J. GOEBEL, *ibid.* p. 277.
256. C. G. RHODES, C. C. BAMPTON and J. A. GRAVES, *ibid.* p. 349.
257. A. M. RITTER, E. L. HALL and N. LEWIS, *ibid.* p. 413.
258. J. A. DEKOCK, Y. A. CHANG, M-X. ZHANG and O. Y. CHEN, in "Interfaces in Composites", Series **170**, edited by C. G. Pantano and E. J. Chen (MRS, Pittsburgh, 1990) p. 173.
259. D. R. BAKER, P. J. DOORBAR and M. H. LORETTO, *ibid.* p. 85.
260. C. J. YANG, S. M. JENG and J-M. YANG, *Scripta Metall.* **24** (1990) 469.
261. J. I. ELDRIDGE and P. K. BRINDLEY, *J. Mater. Sci. Lett.* **8** (1989) 1451.
262. A. K. MISRA, in "Interfaces in Metal–Ceramic Composites", edited by R. Y. Lin, R. J. Arsenault, G. P. Martins and S. G. Fishman (TMS, Warrendale, Pennsylvania, 1990) p. 85.
263. S.M. RUSS, *Met. Trans.* **21A** (1990) 1595.
264. M. KHAIRUL ALAM and S. C. JAIN, *JOM* **42**(11) (1990) 56.
265. S. KRISHNAMURTHY and P. R. SMITH, WPAFB, Ohio, Private Communication (1991).
266. C. M. WARD-CLOSE and P. G. PARTRIDGE, *J. Mater Sci.* **25** (1990) 4315.
267. M. L. GAMBONE, WRDC-TR-89-4145, Vols 1 and 2 (WPAFB, Ohio, 1989).
268. K. R. BAIN, M. L. GAMBONE and R. D. ZORDAN, in "Intermetallic Matrix Composites", series Vol. 194, edited by D. L. Anton, P. L. Martin, D. B. Miracle and R. McMeeking (MRS, Pittsburgh, 1990) p. 271.
269. P. R. SMITH and W. C. REVELOS, in"Fatigue '90", Vol. 3, edited by H. Kitagawa and T. Tanaka (Materials & Components Engineering, Birmingham, UK, 1990) p. 1711.
270. P. K. BRINDLEY, P. A. BARTOLOTTA and R. A. MACKAY, "HITEMP Review 1989 – Advanced High Temperature Engine Materials Technology Program", Report CP-10039 (NASA, Lewis, Cleveland, Ohio, 1989) p. 52-1.
271. L. CHRISTODOULOU and J. M. BRUPBACHER, *Mater. Edge* **7** (November/December 1990) 29.
272. L. CHRISTODOULOU, P. A. PARRISH and C. R. CROWE, in "High Temperature/High Performance Composites", series Vol. 120, edited by F. D. Lemkey, A. G. Evans, S. G. Fishman and J. R. Strife (MRS, Pittsburgh, 1988) p. 29.
273. M. L. ADAMS, S. L. KAMPE, A. R. HARMON and L. CHRISTODOULOU, in "Advances in Powder Metallurgy", edited by T. G. Gasbarre and W. F. Jandeska Jr (MPIF, Princeton, 1989) p. 439.
274. S. L. KAMPE, J. A. CLARKE and L. CHRISTODOULOU, in "Intermetallic Matrix Composites", series Vol. 194, edited by D. L. Anton, P. L. Martin, D. B. Miracle and R. McMeeking (MRS, Pittsburgh, 1990) p. 225.
275. D. E. LARSEN, Jr. S. L. KAMPE and L. CHRISTODOULOU, *ibid.* p. 285.
276. D. E. LARSEN, M. L. ADAMS, S. L. KAMPE, L. CHRISTODOULOU and J. D. BRYANT, *Scripta Metall.* **24** (1990) 851.
277. O. POPOOLA, C. CORDIER, P. PIROUZ and A. H. HEUER, in "Interfaces in Metal–Ceramic Composites", edited by R. Y. Lin, R. J. Arsenault, G. P. Martins and S. G. Fishman (TMS, Warrendale, Pennsylvania, 1990) p. 465.
278. T. CHRISTMAN, A. NEEDLEMAN and S. SURESH, *Acta Metall.* **37** (1989) 3029.
279. J. RÖSLER, J. J. VALENCIA, C. G. LEVI, A. G. EVANS and R. MEHRABIAN, in "Intermetallic Matrix Composites", series Vol. 194, edited by D. L. Anton, P. L. Martin, D. B. Miracle and R. McMeeking (MRS, Pittsburgh, 1990) p. 241.
280. D. DIX, *Defense News* (July 16 1990) 7.
281. D. DRIVER, in "High Temperature Materials for Power Engineering", Part II, edited by E. Bachelet and D. Driver (Kluwer, The Netherlands, 1990) p. 883.
282. T. M. F. RONALD, *Adv. Mater. Process.* **135**(5) (1989) 29.
283. V. P. McCONNELL, *Adv. Compos.* (November/December 1990) 37.
284. J. STRINGER, *Acta Metall.* **8** (1969) 758.
285. P. H. MORTON and W. M. BALDWIN, *Trans. ASM* **44** (1952) 1004.
286. A. E. JENKINS, *J. Inst. Metals* **84** (1955) 1.
287. P. KOFSTAD, *J. Less-Common Metals* **12** (1967) 449.
288. D. ELIEZER, University of Idaho, Moscow, Idaho, Work in Progress (1991).
289. Y. UMAKOSHI, M. YAMAGUCHI, T. SAKAGAMI and T. YAMANE, *J. Mater. Sci.* **24** (1989) 1599.
290. M. SIMMOND, A. SPILNERS and O. KATZ, *J. Metals* **7** (1955) 645.
291. C. S. GIGGINS and F. S. PETTIT, *J. Electrochem. Soc.* **118** (1971) 1782.
292. S. KROL and T. GORECKI, in "Titanium Science and Technology", Vol. 4, edited by G. Lutjering, U. Zwicker and W. Bunk (DGM, Oberursel, Germany, 1985) p. 2695.
293. A. M. CHAZE, C. CODDET and G. BERANGER, *J. Less-Common Metals* **83** (1982) 49.
294. V. V. GLAZOVA, *Russian Metall.* No. 2 (1967) 116.
295. D. V. IGNOTOV, Z. I. KORNILOVA, E. M. LAZAVER and V. M. POPOVA, *ibid.* No. 2 (1972) 150.
296. G. WELSCH and A. I. KAHVECI, in "Environmental Degradation of Engineering Materials III", edited by M. R. Louthan Jr, R. P. McNitt and R. D. Sisson Jr (Pennsylvania State University, University Park, Pennsylvania, 1987) p. 47.
297. A. I. KAHVECI, G. WELSCH and G. E. WASIELEWSKI, in Proceedings of 6th World Conference on Titanium, Vol. 2, Cannes, France, June 1988, edited by P. Lacombe, R. Tricot and G. Beranger (Les Editions de Physique, Les Ulis Cedex, France, 1989) p. 1015.
298. S. J. BALSONE, in "Oxidation of High Temperature Intermetallics", edited by T. Grobstein and J. Doychak (TMS-AIME, Warrendale, Pennsylvania, 1989) p. 219.
299. S. J. BALSONE, T. NICHOLAS, D. C. MAXWELL and M. KHOBAIB, in "Elevated Temperature Crack Growth",

edited by S. Mall and T. Nichols (American Society for Mechanical Engineering, New York, 18, 1990) p. 87.

300. M. KABBAJ, A. GALERIE and M. CAILLET, *J. Less-Common Metals* **108** (1985) 1.

301. D. S. SHIH, G. K. SCARR and G. E. WASIELEWSKI, *JOM* **39**(7) (1987) 7.

302. D. E. MATEJCZYK and R. P. JEWETT, in Proceedings of the 2nd NASP Hydrogen Materials Interaction Workshop, Publication No. 1004, edited by H. G. Nelson (NASA, Moffett Field, California, 1988) p. 137.

303. T. FOX, D. B. KNORR and N. S. STOLOFF, Rensselaer Polytechnic Institute, Troy, New York, Unpublished Work (1989).

304. D. ELIEZER and F. H. FROES, University of Idaho, Moscow, Idaho, work in progress.

305. J. H. HOLBROOK, H. J. CIALONE and B. S. MAJUMDAR, in Proceedings of 3rd NASP Hydrogen Materials Interactions, edited by H. G. Nelson (NASA, Moffett Field, California, 1989) in press.

306. W. Y. CHU, A. W. THOMPSON and J. C. WILLIAMS, in "Hydrogen Effects on Materials Behavior", edited by N. R. Moody and A. W. Thompson (TMS, Warrendale, Pennsylvania, 1990) p. 543.

307. M. GAO, J. B. BOODEY and R. P. WEI, *Scripta Met. Mater.* **24** (1990) 2135.

308. D. ELIEZER, E. MANOR and F. H. FROES, in "Hydrogen Effects on Materials Behavior", edited by N. R. Moody and A. W. Thompson (TMS, Warrendale, Pennsylvania, 1990) p. 523.

309. E. MANOR and D. ELIEZER, *Scripta Metall.* **23** (1989) 1313.

310. *Idem, Scripta Met. Mater.* **24** (1990) 129.

311. H. G. NELSON, in "Space Age Metals Technology", edited by F. H. Froes and R. A. Cull (SAMPE, Covina, California, 1988) p. 310.

312. L. G. FRITZEMEIR and M. A. JACINTO, in "Hydrogen Effects on Materials Behavior", edited by N. R. Moody and A. W. Thompson (TMS, Warrendale, Pennsylvania, 1990) p. 533.

313. A. A. SHEIMKER and S. M. EL-SOUDANI, in Proceedings of 3rd NASP Hydrogen Materials Interactions, edited by H. G. Nelson (NASA, Moffett Field, California, 1989) in press.

314. D. E. MATEJCZYK and C. G. RHODES, *Scripta Met. Mater.* **24** (1990) 1369.

315. L. CHRISTODOULOU and J. A. CLARKE, in "Hydrogen Effects on Materials Behavior", edited by N. R. Moody and A. W. Thompson (TMS, Warrendale, Pennsylvania, 1990) p. 515.

316. F. H. FROES, J. J. deBARBADILLO and C. SURYANARAYANA, in "Structural Applications of Mechanical Alloying", edited by F. H. Froes and J. J. deBarbadillo (ASM International, Materials Park, Ohio, 1990) p. 1.

317. R. N. HADCOCK, *J. Aircraft* **17**(9) (1980) 609.

318. B. DOGAN, "Intermetallic Alloys: Deformation, Mechanical and Fracture Behavior", Report 88/E/53 (GKSS-Forschungszentrum Geesthacht GmBH, Germany, 1988).

319. B. DOGAN, R. WAGNER and P. A. BEAVEN, *Scripta Met. Mater.* **25** (1991) 773.

320. Y. NISHIYAMA, T. MIYASHITA, S. ISOBE and T. NODA, in "High-Temperature Aluminides and Intermetallics", edited by S. H. Whang, C. T. Liu, D. P. Pope and J. O. Stiegler (TMS, Warrendale, Pennsylvania, 1990) p. 557.

321. R. DELAGI (TI, Attleboro, Massachusetts), Private Communications (1990).

322. C. BASSI, J. A. PETERS and J. WITTENAUER, *JOM* **41**(9) (1989) 18.

323. N. MASAHASHI, M. MATSUO, Y. MIZUHARA, M. KIMURA and K. HASHIMOTO, in "Microstructure/Property Relationships in Titanium Alloys and Titanium Aluminides", edited by Y-W. Kim and R. R. Boyer (TMS, Warrendale, Pennsylvania, 1991) in press.

324. K. HASHIMOTO, N. MASAHASHI, Y. MIZUHARA, H. FUJII and M. MATSUO, *ibid.*

325. J. C. WILLIAMS and L. A. JOHNSON, GE/Aircraft Engines, Evendale, Ohio, Private Communication (1990).

326. D. P. DeLUCA and B. A. COWLES, WRDC-TR-89-4136 (WPAFB, Ohio, 1989).

327. J. LINCOLN, in 14th Symposium of International Committee on Aeronautical Fatigue, edited by D. L. Simpson (Engineering Materials Advisory Services, Warley, W. Midlands, UK, 1987) p. 619.

328. H. A. LIPSITT, in "Advanced High Temperature Alloys: Processing and Properties", edited by S. S. Allen, R. M. Pelloux and R. Widmer (ASM, Metals Park, Ohio, 1986) p. 157.

329. E. K. HOFFMAN, R. K. BIRD and T. T. BALES, in "Light-Weight Alloys for Aerospace Applications", edited by E. H. Chia and N. J. Kim (TMS-AIME, Warrendale, Pennsylvania, 1989) p. 481.

Received 21 May
and accepted 25 July 1991